

19930093563 A-54
ACR No. 4A15

NATIONAL ADVISORY COMMITTEE FOR AERONAUTICS

WARTIME REPORT

ORIGINALLY ISSUED

January 1944 as
Advance Confidential Report 4A15

WIND-TUNNEL INVESTIGATION OF AILERONS ON A
LOW-DRAG AIRFOIL. II - THE EFFECT OF
THICKENED AND BEVELED TRAILING EDGES

By Robert M. Crane and Ralph W. Holtzclaw

Ames Aeronautical Laboratory
Moffett Field, California



WASHINGTON

NACA WARTIME REPORTS are reprints of papers originally issued to provide rapid distribution of advance research results to an authorized group requiring them for the war effort. They were previously held under a security status but are now unclassified. Some of these reports were not technically edited. All have been reproduced without change in order to expedite general distribution.

NATIONAL ADVISORY COMMITTEE FOR AERONAUTICS

ADVANCE CONFIDENTIAL REPORT

WIND-TUNNEL INVESTIGATION OF AIILRONS ON A
LOW-Drag AIRFOIL. II - THE EFFECT OF
THICKENED AND BEVELED TRAILING EDGES

By Robert M. Crane and Ralph W. Holtzclaw

SUMMARY

An investigation was made in the Ames Aeronautical Laboratory 7- by 10-foot wind tunnel of the effects of modifications to the trailing edge of a 0.20-chord plain sealed aileron on an NACA 66,2-216 ($a = 0.6$) airfoil. The modifications considered consisted of various amounts of symmetrical thickening and beveling of the aileron trailing edge. Aileron control characteristics were estimated for two high-speed airplanes equipped with normal-profile ailerons and with the modified ailerons.

Thickening and beveling the trailing edge of the aileron was found to reduce the aileron effectiveness, reduce the slope of the wing section lift curve, and reduce the hinge-moment coefficients. These effects were maximum for the bevel, the length of which was 20 percent of the aileron chord, and decreased for both increasing and decreasing bevel lengths. Thickening and beveling the trailing edge caused an increase of 0.0001 in the minimum profile-drag coefficient.

The optimum beveled trailing edge on a typical aileron installation caused a reduction of 50 percent in the control force for a large rate of roll at high speed. When used in conjunction with internal balance, the thickened and beveled profile resulted in a 30-percent reduction in the nose balance required for a given control force at high speed. Under these conditions the variation of control force with rate of roll was more nearly linear for the aileron of normal profile than for the ailerons with thickened and beveled trailing edges.

INTRODUCTION

With every increase in size and speed of modern high-performance airplanes, the problem of attaining adequate lateral control without excessive control forces becomes less amenable to solution by simple aerodynamic balancing methods. Of the various methods of aerodynamic balance available, one of the most efficient is the sealed internal nose balance. However, sufficient control lightness frequently cannot be satisfactorily attained by the use of an internal nose balance alone. The necessary balance may be so large that the required control-surface deflection cannot be obtained, or structural necessities of the main surfaces may be such that adequate balance cannot be incorporated in the design. Aileron profile offers an independent means of adjusting aileron hinge moments without the additional linkages and loss in effectiveness associated with a balancing tab. Reference 1 has presented the aerodynamic effects of thinning and thickening the control-surface profile. Two-dimensional flow tests on an NACA 0009 airfoil (reference 2) and three-dimensional flow tests on a tapered NACA 230-series wing (reference 3) and on a tapered low-drag wing (reference 4) indicate that thickening and beveling the control-surface trailing edge is a powerful means of adjusting hinge-moment characteristics.

The purpose of the tests reported herein was to obtain quantitative data on the effect of thickened and beveled trailing edges on the characteristics of ailerons on a low-drag airfoil in two-dimensional flow.

MODEL AND APPARATUS

Model

The airfoil used in these tests was constructed of laminated mahogany to the NACA 66,2-216 ($a = 0.6$) profile of 4-foot chord and 5-foot span. The airfoil ordinates are given in table I. The ailerons were constructed of laminated mahogany and had a nose-gap seal of dental rubber dam. The aileron ordinates are given in table II. The ordinates of the normal-profile aileron are the same as the corresponding ordinates of the NACA 66,2-216 ($a = 0.6$) airfoil. The details of the ailerons, and the

modifications tested, are shown in figure 1. The method of determining the profile of the thickened and beveled trailing edges is described in the appendix. Since, as shown in figure 1, beveling the trailing edge was necessarily accompanied by a definite amount of thickening, the modified profiles are for simplicity hereafter referred to as beveled trailing-edge ailerons and beveling the trailing edge is understood to mean thickening and beveling as shown by the figure.

Test Installation

The airfoil was mounted vertically in the test section of the AAL 7- by 10-foot wind tunnel No. 1, as shown in the photographs of figure 2. End plates were attached to the 5-foot-span section. Fairings of the same airfoil section as the wing were fastened to the tunnel floor and ceiling turntables and were used to shield the connections between the model and the balance frame. These fairings were not equipped with ailerons. Provisions were made for changing the angle of attack and the aileron angle while the tunnel was in operation. Aileron hinge moments were measured by means of electrical resistance-type strain gages which were mounted on a member which restrained the torque tube of the aileron from rotation.

COEFFICIENTS AND CORRECTIONS

The coefficients used in the presentation of results follow:

c_l airfoil section lift coefficient (l/qc)

c_d_0 airfoil section profile-drag coefficient (d_0/qc)

c_m airfoil section pitching-moment coefficient (m/qc^2)

c_h aileron section hinge-moment coefficient (h/qc_a^2)

P/q internal static pressure at aileron nose divided by dynamic pressure (fig. 1)

Δc_l increment of c_l due to deflecting the aileron from neutral

$\Delta c_l'$ c_l of down aileron minus c_l of up aileron

Δc_{d_0} increment of c_{d_0} due to deflecting the aileron from neutral

Δc_h increment of c_h due to deflecting the aileron from neutral

$\Delta c_h'$ c_h of up aileron minus c_h of down aileron

$\Delta P/q$ increment of pressure coefficient across aileron nose seal (pressure below seal minus pressure above seal divided by dynamic pressure)

where

l airfoil section lift

d_c airfoil section profile drag

m airfoil section pitching moment about quarter-chord of airfoil

h aileron section hinge moment

c chord of airfoil with aileron neutral

c_a chord of aileron aft of aileron hinge line

q dynamic pressure of air stream ($1/2 \rho V^2$)

V free-stream velocity

In addition to the preceding, the following symbols are employed:

α_0 angle of attack for airfoil of infinite aspect ratio

δ_a aileron deflection with respect to the airfoil

b wing span of assumed airplane

v_i indicated airspeed, miles per hour

p rate of roll, radians per second

$$c_{l\alpha} = (\partial c_l / \partial \alpha)_{\delta_a=0^\circ} \quad (\text{measured through } \alpha_0 = 0^\circ)$$

$$c_{l\delta_a} = (\partial c_l / \partial \delta_a)_{\alpha_0=0^\circ} \quad (\text{measured through } \delta_a = 0^\circ)$$

$$c_{h\alpha} = (\partial c_h / \partial \alpha)_{\delta_a=0^\circ} \quad (\text{measured through } \alpha_0 = 0^\circ)$$

$$c_{h\delta_a} = (\partial c_h / \partial \delta_a)_{\alpha_0=0^\circ} \quad (\text{measured through } \delta_a = 0^\circ)$$

The subscripts outside the parentheses represent the factors held constant during the measurement of the parameters.

The lift coefficient, profile-drag coefficient, and pitching-moment coefficient have been corrected for tunnel-wall effects. Section profile drag was determined by measurement of loss of momentum in the wing wake. A comparison of force-test and pressure-distribution measurements of section lift coefficient and section pitching-moment coefficient indicated that the end plates had no effect on these coefficients with the aileron neutral. No corrections have been applied to section hinge-moment coefficients and no end-plate correction has been applied to Δc_l . Because of possible tip losses, it is believed that the measured aileron effectiveness is slightly low and rates of roll computed from these data will be conservative. By comparison of these data with section data on a similar airfoil (reference 5), it is estimated that the decrease in the value of Δc_l due to this effect is not more than 12 percent.

TESTS

For each of the aileron profile modifications, two series of tests were made. The first series obtained aileron characteristics at the highest Reynolds number obtainable (9,000,000) at five angles of attack (-4° , -2° , 0° , 2° , and 4°). A second series, at angles of

attack of 0°, 4°, 8°, and 12°, was run at a reduced Reynolds number (3,800,000). With the aileron neutral, section characteristics were obtained at a Reynolds number of 8,200,000. Section profile-drag coefficients were obtained with the aileron neutral, at the ideal lift coefficient ($c_l = 0.21$), over a Reynolds number range of 3,000,000 to 10,000,000.

RESULTS AND DISCUSSION

Basic section data.- The basic section data, with aileron deflected and aileron neutral, are presented in figures 3 to 9. These data may be utilized to predict the section characteristics of ailerons with any amount of internal nose balance by means of the equation

$$(c_h)_B = c_h + \Delta P/q \frac{(B^2 - R^2)}{2}$$

where

$(c_h)_B$ aileron section hinge-moment coefficient of aileron with sealed internal nose balance

c_h aileron section hinge-moment coefficient of plain aileron

B nose balance (expressed as fraction of c_a)

R nose radius of plain aileron (expressed as fraction of c_a)

While these basic data are useful for purposes of aileron design, the prediction and comparison of the effects of aileron profile on section characteristics may be more conveniently demonstrated by means of section parameters. For this purpose, plots showing the relation of various coefficients and parameters to other independent variables have been prepared.

Aileron effectiveness.- The effect of the beveled trailing edge on the aileron-effectiveness parameter $(\partial\alpha/\partial\delta_a)_{c_n}$ is shown in figure 11. The value of this

parameter for the normal-profile aileron is, at a Reynolds number of 9,000,000, about 71 percent of that which would be predicted from thin-airfoil theory and about 90 percent of the value obtained on the NACA 0009 airfoil (reference 6). The effect of beveling the trailing edge was to reduce the value of $(\partial \alpha / \partial \delta_a)_{\text{ch}}$ by about 10 percent.

Beveling the trailing edge had a similar influence on effectiveness at the higher aileron deflections, where the flow over the aileron has separated. Figure 12 represents the total $\Delta c_l'$ available due to 30° of total aileron deflection, plotted against angle of attack. At moderate angles of attack ($\alpha_0 = -4^\circ$ to 4°), beveling the trailing edge caused a 14-percent reduction in the $\Delta c_l'$ available, but at $\alpha_0 = 12^\circ$ there is only a minor variation of $\Delta c_l'$ for the various trailing-edge profile alterations. The deleterious effects of trailing-edge bevel on aileron effectiveness were a maximum for the $0.20c_a$ bevel and decreased for both increasing and decreasing bevel lengths.

To determine the effect of beveled trailing edges on the aileron effectiveness of a typical installation, these data have been applied to the prediction of the aileron control characteristics of a typical pursuit airplane and a medium bomber. The airplane data necessary for the calculations are presented in table III. The calculations have been made assuming zero sideslip of the airplane and no torsional deflection of the wing. The effect of aileron profile on c_{l_a} has been included in the determination of C_{l_p} , the damping moment coefficient due to rolling. The calculated variation of $pb/2V$, with total aileron deflection for the various aileron profiles is presented in figures 13 and 14 for indicated airspeeds of 300 and 120 miles per hour. Examination of these figures reveals that the aileron effectiveness at low speeds was little influenced by aileron trailing-edge profile. Thus the size and the total aileron deflection for an installation of given effectiveness would be unchanged by control-surface profile modifications at the trailing edge.

Aileron hinge moments.—The effect of the beveled trailing edge on the aileron hinge-moment parameter ch_{δ_a} is shown in figure 15, and a comparison is afforded between these experimental values, the theoretical value

from thin-airfoil theory and the experimental value obtained on an NACA 0009 airfoil (reference 6). Beveling the aileron trailing edge results in an algebraic increase in $c_{h\delta_a}$. The variation, with angle of attack,

of the total $\Delta c_h'$ due to 30° of total aileron deflection is presented in figure 16. The beveled trailing edge reduces the value of $\Delta c_h'$, but at large angles of attack the effect is very small. Comparative curves of c_h against δ_a for the various bevel lengths are presented in figure 17. The balancing effect of the bevel increases with reduction in bevel length to an optimum value with the $0.20c_a$ bevel. For the shorter bevel, the balancing effect is lessened.

Unlike the thickened and thinned aileron profiles reported in reference 1, the presence of the beveled trailing edge had a large effect on the angular range of linear hinge-moment characteristics. At $\alpha_0 = 0^\circ$ this range was reduced from 16° of total aileron deflection for the normal-profile aileron to 3° of total aileron deflection for the $0.20c_a$ bevel. This linear range was a minimum for the $0.20c_a$ bevel, and increased for both increasing and decreasing bevel lengths.

The value of $(\partial c_h / \partial \alpha)_{\delta_a}$ varies with angle of attack and with aileron deflection. At small angles of attack and small aileron deflections, the beveled trailing edge causes a large algebraic increase in $(\partial c_h / \partial \alpha)_{\delta_a}$. The value of $(\partial c_h / \partial \alpha)_{\delta_a} = 0$ in this region varies between -0.0049 for the normal-profile aileron to 0.010 for the $0.00c_a$ bevel. A positive value of $(\partial c_h / \partial \alpha)_{\delta_a}$ will induce an unfavorable response and will tend to increase the effective dihedral and the damping in roll, stick free. As the aileron angle is increased, $(\partial c_h / \partial \alpha)_{\delta_a}$ becomes negative (i.e., the response becomes favorable) for the beveled profiles at the aileron angles at which separation occurs over the ailerons. At angles of attack greater than 6° , $(\partial c_h / \partial \alpha)_{\delta_a} = 0$ has a constant value of -0.010 irrespective of aileron profile.

To determine the effect of nose seal on the beveled trailing-edge profiles, tests at five angles of attack were made on the $0.20c_a$ beveled profile with a 0.25-inch (0.0052_c) nose gap. The data are presented in figure 18.

In addition to the loss in effectiveness usually associated with this condition, the nose gap decreased the hinge moments at low aileron deflections and further decreased the angular range of linear hinge-moment characteristics. Because of the decreased effectiveness, the unsealed beveled aileron is inferior to the sealed beveled aileron as a means of reducing control forces.

The data of figures 3 to 7 have been plotted in figure 19 as hinge-moment parameters against lift parameters. The curves show the relative dependence of the aileron hinge moments on the aileron effectiveness and on the slope of the wing section lift curve. In addition to the data shown for the ailerons of the present investigation, experimental points are included from data obtained for a series of 0.20-chord ailerons with thickened and thinned aileron profiles (reference 1). The small deviation of the experimental points from the mean curves indicates that the relationships indicated are little influenced by the chordwise distribution of thickness of the control-surface profile.

Since the effect of aileron profile on $\Delta P/q$ is small, the hinge-moment coefficients of ailerons with internal nose balance will exhibit aileron-profile effects similar to those observed on the plain ailerons. As separation occurs over the aileron at large deflections, there is an abrupt loss in P/q over the suction side of the control (side opposite the deflection). This loss accounts for the nonlinearity of the curves of $\Delta P/q$ against δ_a (figs. 3 to 7). It is this reduction in $\Delta P/q$ which causes the nonlinearity of hinge-moment curves of ailerons with large amounts of internal nose balance. Because of the earlier flow separation of the ailerons with beveled trailing-edge profiles, this nonlinearity is more pronounced for the beveled trailing-edge profiles than it is for the normal profile.

Aileron control forces. - The effect of beveled trailing edges on aileron control characteristics may be evaluated from two considerations: the reduction in control force due to the bevel when the aileron is designed with a given aerodynamic nose balance, and the reduction in nose balance due to the bevel when the aileron is designed for a given control force.

Figures 20 to 23 illustrate the changes in control-force characteristics which result from a beveled trailing edge. The airplane data necessary for these calculations

are presented in table III. For the pursuit airplane, the ailerons are selected with 0.40ca aerodynamic nose balance, and for the medium bomber no nose balance is used. At a $pb/2V$ of 0.08 at high speed, the 0.30ca bevel causes a 70-pound reduction in stick force for the pursuit airplane and an 80-pound reduction in wheel force for the medium bomber. At low speeds the percent reduction in control force due to the bevel is less. This is caused by the previously mentioned reduction in bevel effect on hinge moments at large angles of attack. The effect of the trailing-edge bevel on the angular range of linear control characteristics is further emphasized by figures 20 and 22. While the variation of control force with $pb/2V$ is linear for the airplane equipped with normal-profile ailerons to a $pb/2V$ of 0.07, the linear range with the aileron with a 0.20ca bevel (sealed) extends only to a $pb/2V$ of 0.035. The removal of the nose seal on the 0.20ca bevel aileron further reduces this range to a $pb/2V$ of 0.02.

Figures 24 to 27 present the variation of control force with $pb/2V$ when each aileron has an assumed nose balance such that a $pb/2V$ of 0.08 can be attained with a stick force of 30 pounds at 380 miles per hour on the pursuit airplane and a wheel force of 80 pounds at 250 miles per hour on the medium bomber.

For the pursuit airplane under consideration, the 0.40ca, 0.20ca, and 0.10ca beveled trailing-edge ailerons are overbalanced for moderate values of $pb/2V$ at $V_i = 300$ miles per hour. This overbalance is a result of the reduced linear range of hinge-moment coefficient against aileron deflection due to the beveled trailing edge and the reduced effectiveness of the beveled profiles. Another contributing factor to the overbalance is the fact that the addition of the bevel causes a larger reduction in $\Delta P/q$ at large aileron deflection than it does at small aileron deflection. This difference increases the effectiveness of the internal balance at the aileron deflections corresponding to low rates of roll and thus contributes to the overbalance. These deleterious effects are partially compensated for by the reduced balance required with the beveled profiles and the presence of an unfavorable response at low aileron deflections and a favorable response at high aileron deflections, both factors tending to increase the linearity of stick force against $pb/2E$. While the aileron with 0.30ca bevel is not overbalanced, the

variation of stick force with $pb/2V$ is not as nearly linear as is the gradient attainable with the normal-profile aileron. The aileron with $0.30ca$ bevel requires 13-percent ca less nose balance than is required of the normal-profile aileron. This reduced nose balance may be advantageous for structural reasons and it will reduce the lift loads on the aileron structure. The value of ch_{δ_a} for this $0.30ca$ bevel aileron with $0.40ca$ nose balance is 0.0015. In a steady roll this positive value of ch_{δ_a} is of no importance due to the unfavorable response (positive $(\partial ch/\partial \alpha)_{\delta_a}$) of the ailerons. In level flight, stick free, there may be some oscillations of the ailerons due to the positive value of ch_{δ_a} .

When applied to the medium bomber, the bevel has an equally large effect on the wheel-force gradient and the nose balance required for a high-speed wheel force of 80 pounds for a $pb/2V$ of 0.08. When designed for this condition, the required nose balance varies from $0.455ca$ for the normal-profile aileron to $0.296ca$ for the aileron with $0.30ca$ bevel. The effect on high-speed wheel-force gradient is such that the control force necessary to attain a $pb/2V$ of 0.06 varies from 54 pounds for the normal profile to 25 pounds for the $0.40ca$ bevel profile. At low speeds the control force is increased due to the presence of the bevel. This effect is due to the reduced nose balance required of the beveled contours.

Lift.— Thickening and beveling the aileron trailing-edge profile caused a decrease in $c_{l\alpha}$. This is shown in figure 8. The effect was maximum for the $0.20ca$ bevel and decreased for both increasing and decreasing bevel lengths.

Pitching moment.— Beveling the aileron trailing edge caused an increase in $(\partial c_m/\partial c_l)_{\delta_a=0}$ corresponding to a forward shift of the aerodynamic center. This is shown in figure 8.

Drag.— Figure 10 presents the variation of section profile drag coefficient with Reynolds number at the ideal lift coefficient ($c_l = 0.21$). The presence of the aileron-bevel caused an increase in c_{d_0} of 0.0001. The straight-sided aileron profile (reference 1) resulted in a profile-drag coefficient increase of 0.0004, indicating that the effect of a profile discontinuity on profile drag decreases as the discontinuity approaches the trailing edge of the airfoil.

Reynolds number.— Examination of figures 3 to 7 reveals that, at small angles of attack increasing Reynolds number resulted in a loss in $\Delta c_l'$, $\Delta c_h'$, and $\Delta P/q$. The magnitude of these effects of increasing Reynolds number was a maximum for the 0.20 c_a bevel and decreased for both increasing and decreasing bevel lengths. Measurement of the airfoil boundary-layer profiles indicated that these effects were caused by a forward movement of the transition point due to increasing Reynolds number. This forward movement of transition, resulting in a thickening of the boundary layer at the beginning of pressure recovery, results in a less complete recovery, thus causing a decrease in effectiveness, hinge moment, and $\Delta P/q$.

CONCLUSIONS

The results of the tests of the 0.20-chord aileron on a low-drag wing indicate that the following conclusions may be drawn:

1. Beveling the aileron trailing edge causes a decrease in aileron effectiveness, a decrease in the slope of the wing section lift curve, a decrease in hinge-moment coefficients, and a reduction in the angular range of linear aileron characteristics. These effects are maximum for the bevel, the length of which is 20 percent of the aileron chord, and decrease for both increasing and decreasing bevel lengths.
2. The magnitude of these bevel effects decreases with increasing angle of attack.
3. The bevels cause an increase of 0.0001 in minimum profile-drag coefficient.

4. The beveled trailing edge causes a reduction of 50 percent in the high-speed control forces for large rates of roll.

5. When used in conjunction with internal nose balance, the trailing-edge bevel results in a 30-percent reduction in the nose balance required for a given control force at high speed.

6. When designed for a given high-speed control force at large rates of roll, the variation of control force with rate of roll is more nearly linear for the aileron of normal profile than for the bevel-profile ailerons. Under these conditions the bevel results in a 50-percent increase in the control force for full deflection at low speed.

7. The changes in slope of the curves of hinge-moment and lift coefficient with respect to angle of attack (due to beveling the aileron) will cause some changes in airplane stability characteristics.

Ames Aeronautical Laboratory,
National Advisory Committee for Aeronautics,
Moffett Field, Calif.

REFERENCES

1. Crane, Robert M., and Holtzclaw, Ralph W.: Wind-Tunnel Investigation of Ailerons on a Low-Drag Airfoil. I - The Effect of Aileron Profile. NACA ACR No. 4A14, Jan. 1944.
2. Jones, Robert T., and Ames, Milton B., Jr.: Wind-Tunnel Investigation of Control-Surface Characteristics. V - The Use of a Beveled Trailing Edge to Reduce the Hinge Moment of a Control Surface. NACA ARR, March 1942.

3. Rogallo, F. M., and Purser, Paul E.: Wind-Tunnel Investigation of a Plain Aileron with Various Trailing-Edge Modifications on a Tapered Wing. II - Ailerons with Thickened and Beveled Trailing Edges. NACA ARR, Oct. 1942.
4. Purser, Paul E., and McKee, John W.: Wind-Tunnel Investigation of a Plain Aileron with Thickened and Beveled Trailing Edges on a Tapered Low-Drag Wing. NACA ACR, Jan. 1943.
5. Danaci, H. G., and Bird, J. D.: Wind-Tunnel Test of Ailerons at Various Speeds. II - Ailerons of 0.20 Airfoil Chord and True Contour with 0.60 Aileron-Chord Sealed Internal Balance on the NACA 66,2-216 Airfoil. NACA ACR No. 3F18, June 1943.
6. Ames, Milton B., Jr., and Sears, Richard I.: Determination of Control-Surface Characteristics from NACA Plain-Flap and Tab Data. Rep. No. 721, NACA 1941.

APPENDIX

The method of determining the thickened and beveled profiles is outlined below:

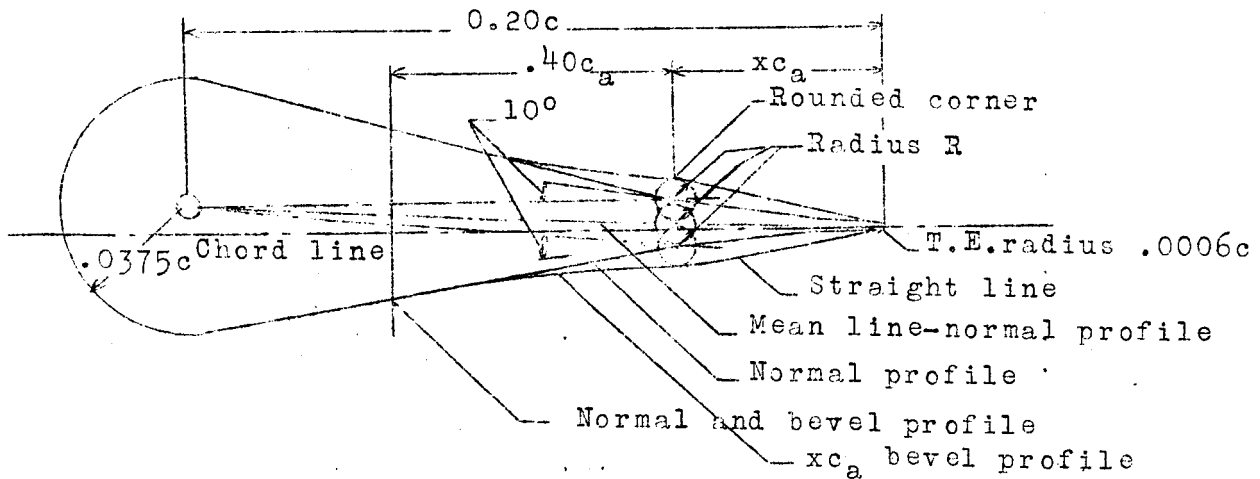
1. At the chordwise station defining the bevel, a perpendicular was erected.
2. With the intersection of the mean line of the normal profile and the perpendicular as a center, a circle was constructed.
3. The radius of the circle, r , was such that the intersection of lines drawn from the hinge center of the aileron and the trailing edge of the aileron intersected on the perpendicular at 10° at a distance, r , from the mean line.

4. With these intersections defining their centers two circles of radius, r , were constructed and tangent lines drawn from these circles to the trailing-edge radius.

5. The forward profile was a free fairing for $0.40c_a$ at which point normal profile was regained.

6. The intersection of this fairing and the bevel was slightly rounded but no attempt was made to fix this radius of curvature.

This method of construction was favored because it was assumed that the action of the bevel was similar to that of a balancing tab and it was desired to maintain every variable constant except the length of the bevel. The aileron profile forward of the bevel was faired into the normal profile to eliminate the abrupt change in profile at the hinge line which would result if straight-sided surfaces were used.



Construction of beveled trailing edge ailerons

TABLE I.- NACA 66,2-216 ($a = 0.6$) AIRFOIL

Stations and ordinates are given in percent of the airfoil chord			
Upper surface		Lower surface	
Station	Ordinate	Station	Ordinate
0	0	0	0
.371	1.242	.629	-1.112
.607	1.501	.893	-1.319
1.091	1.886	1.409	-1.608
2.317	2.615	2.683	-2.127
4.794	3.701	5.206	-2.869
7.234	4.563	7.716	-3.441
9.781	5.308	10.219	-3.934
14.788	6.500	15.212	-4.702
19.806	7.428	20.194	-5.290
24.832	8.155	25.168	-5.741
29.862	8.708	30.138	-6.080
34.897	9.098	35.103	-6.312
39.936	9.356	40.064	-6.462
44.978	9.471	45.022	-6.523
50.023	9.431	49.977	-6.463
55.073	9.224	54.927	-6.336
60.141	8.800	59.859	-6.048
65.191	8.084	64.809	-5.574
70.198	7.068	69.802	-4.866
75.181	5.889	74.819	-4.037
80.148	4.585	79.852	-3.107
85.106	3.265	84.894	-2.177
90.061	1.937	89.939	-1.235
95.021	0.762	94.979	-4.32
100	0	100	0
L.E. radius := 1.575		T.E. radius := 0.0625	

TABLE II - AILERON ORDINATES

[Stations given are wing stations and ordinates are in percent of the airfoil chord]

Normal profile	Beveled profiles										
	0.40 c_a bevel			0.30 c_a bevel			0.20 c_a bevel				C.110 c_a bevel
Station	Upper	Lower	Station	Upper	Lower	Station	Upper	Lower	Station	Upper	Lower
81.25	4.27	-2.85	81.25	4.27	-2.85	81.25	4.27	-2.85	81.25	4.27	-2.85
83.33	3.77	-2.45	83.33	3.77	-2.45	83.33	3.77	-2.45	83.33	3.77	-2.45
85.42	3.21	-2.07	85.42	3.21	-2.07	85.42	3.21	-2.07	85.42	3.21	-2.07
87.50	2.65	-1.67	87.50	2.71	-1.75	87.50	2.68	-1.72	87.50	2.65	-1.67
89.58	2.08	-1.28	89.58	2.29	-1.48	89.58	2.23	-1.44	89.58	2.10	-1.33
91.67	1.54	-.91	91.67	2.01	-1.41	91.67	1.88	-1.25	91.67	1.67	-1.15
93.75	1.06	-.58	92.00	2.00	-1.40	93.75	1.65	-1.24	93.75	1.38	-1.05
95.83	.63	-.33				94.00	1.64	-1.23	96.00	1.27	-.98
97.92	.31	-.17							98.00	.73	-.58
100	0	0									
T.E. radius:	0.062	Straight line from this station tangent to T.E. radius of 0.062	Straight line from this station tangent to T.E. radius of 0.062	Straight line from this station tangent to T.E. radius of 0.062	Straight line from this station tangent to T.E. radius of 0.062	Straight line from this station tangent to T.E. radius of 0.062	Straight line from this station tangent to T.E. radius of 0.062	Straight line from this station tangent to T.E. radius of 0.062	Straight line from this station tangent to T.E. radius of 0.062	Straight line from this station tangent to T.E. radius of 0.062	Straight line from this station tangent to T.E. radius of 0.062

TABLE III.- CHARACTERISTICS OF ASSUMED AIRPLANES

	Pursuit	Medium bomber
Wing:		
Area, square feet	275	800
Span, feet	41.5	80
Aspect ratio	6.23	8.0
Taper ratio	3:1	2.5:1
Section	66,2-216 (a = 0.6)	66,2-216 (a = 0.6)
Ailerons:		
Span	From 0.50b/2 to tip	From 0.50b/2 to tip
Chord	0.20c	0.20c
Deflection	$\pm 15^\circ$	$\pm 15^\circ$
Airplane:		
Wing loading, pounds per square foot	33.7	50
Aileron differential . . .	1:1	1:1
Stick travel, inches . . .	± 8	—
Control wheel travel . . .	—	$\pm 180^\circ$
Control wheel diameter, inches	—	15

NACA

Fig. 1

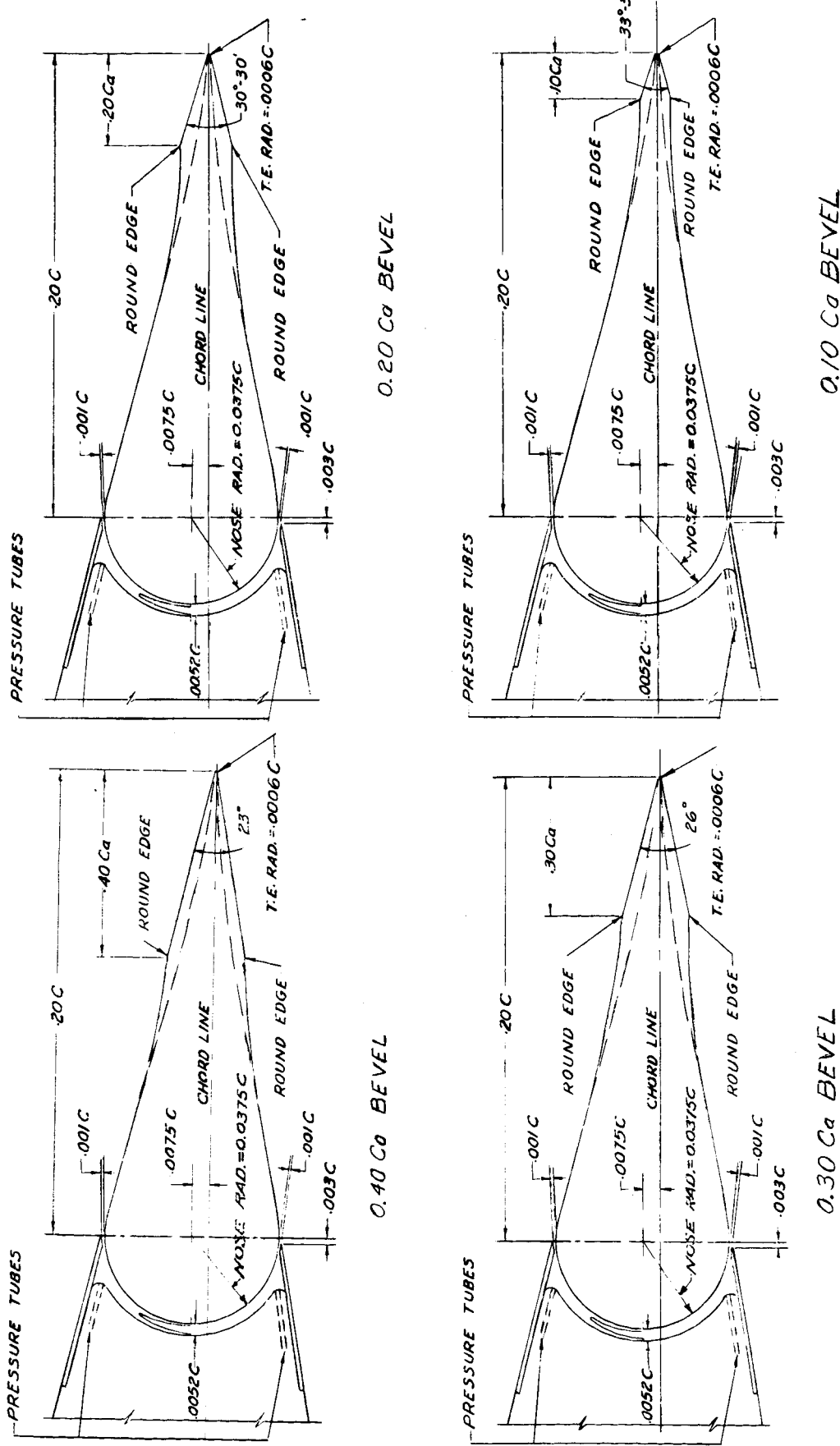


Figure 1.—Thickened and beveled trailing edges on 0.20-chord plain ailerons.

NACA

Fig. 2

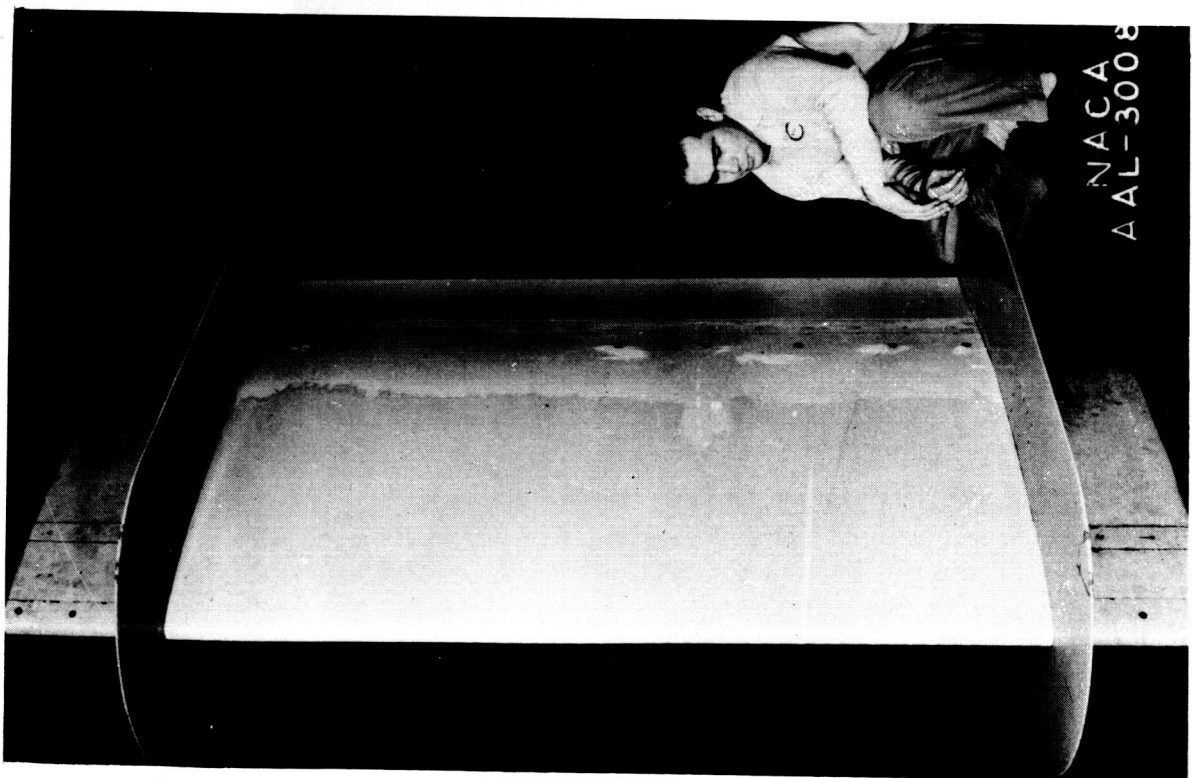
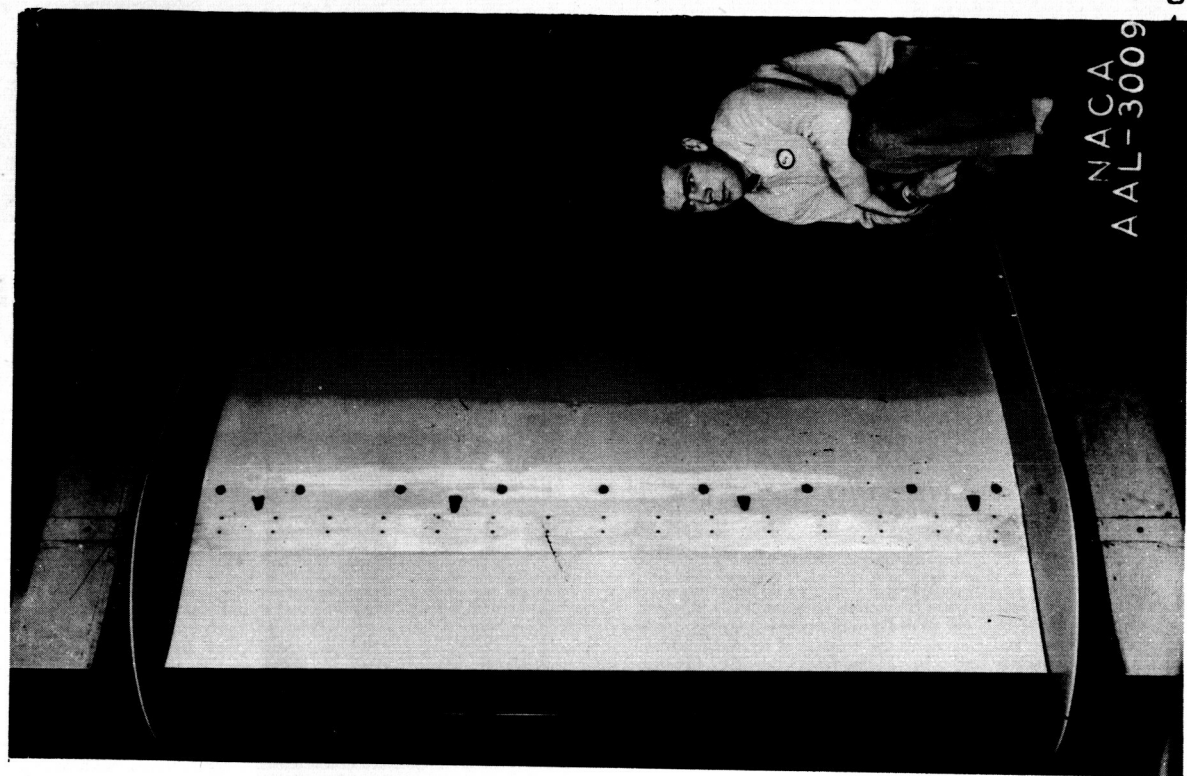


Figure 2.—The NACA 66, 2-216 ($c = 0.6$) airfoil equipped with the 0.20-chord plain aileron of normal profile.

Fig. 3a

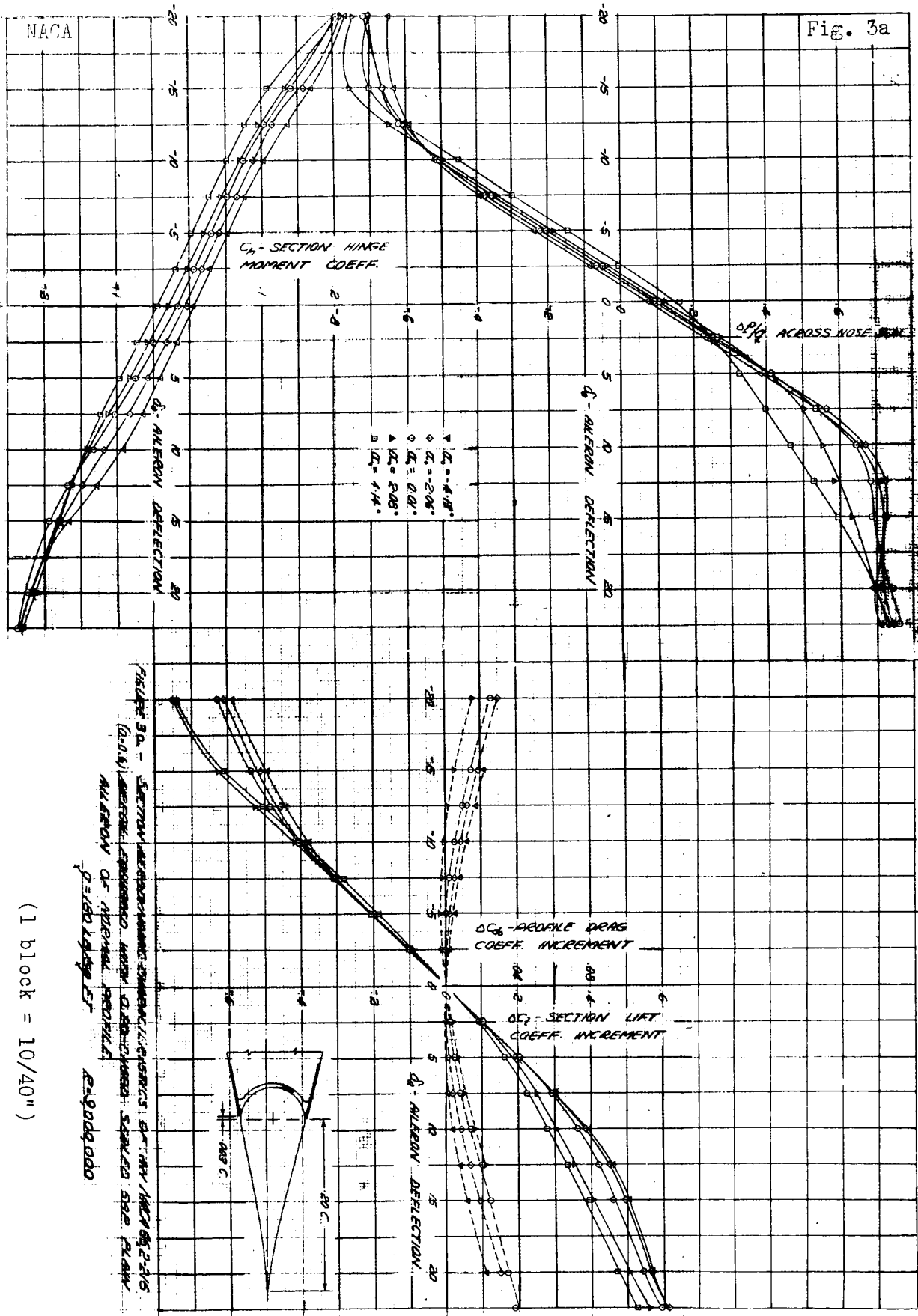
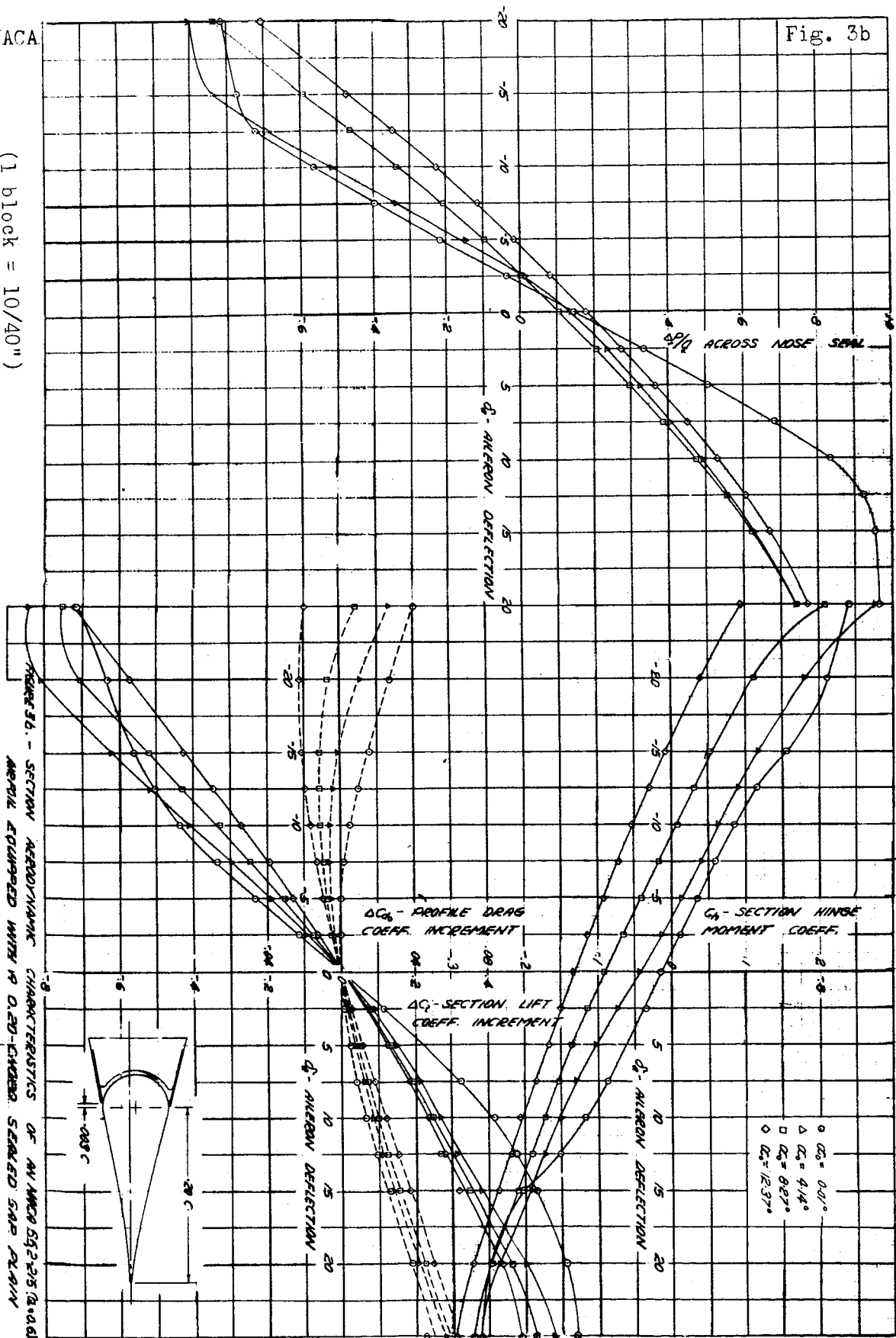


Fig. 3b

NACA

(1 block = 10/40")

FIGURE 3b. - SECTION AERODYNAMIC CHARACTERISTICS OF AN NACA 552-215 (2000) AIRFOIL EQUIPPED WITH A 0.20-CHORD SEATED SWAR PLATE.
 $\rho = 30.19/30$ FT. $P = 9,000,000$

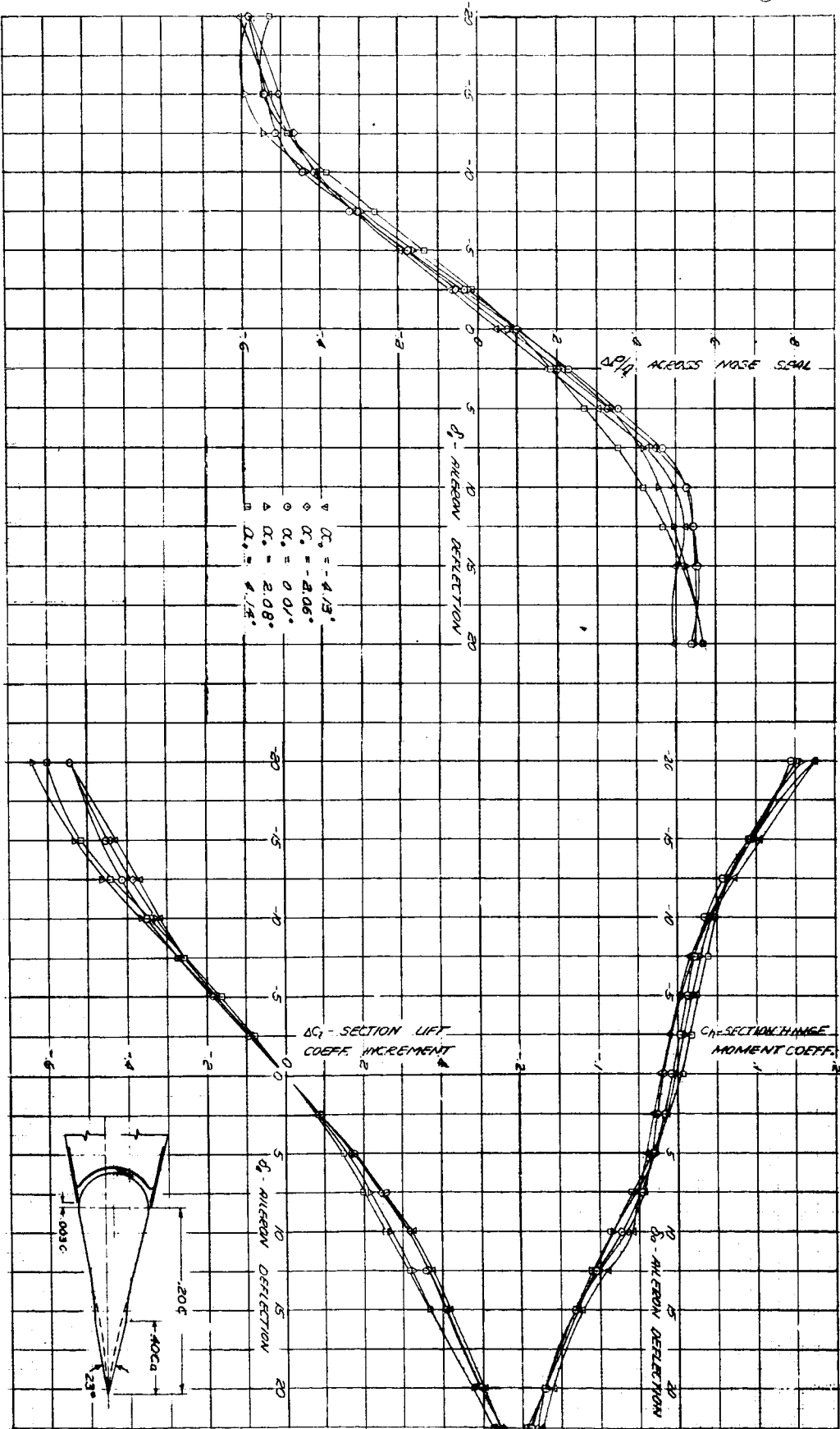


NACA

Fig. 4a

(1 block = 10/40")

PROBLEMS - SECTION AERODYNAMIC CHARACTERISTICS OF NACA 0012-2105
($Q = 0.6$) AIRFOIL EQUIPPED WITH A 0.10 C. CHORD SEMICIRCULAR GAP PLATE.
AIRCRAFT WITH A 0.10 C. REVERSED TAILWING POSITION
 $R = 1800$, $R_{\infty} = 100000$, $\alpha = 2.00000$.

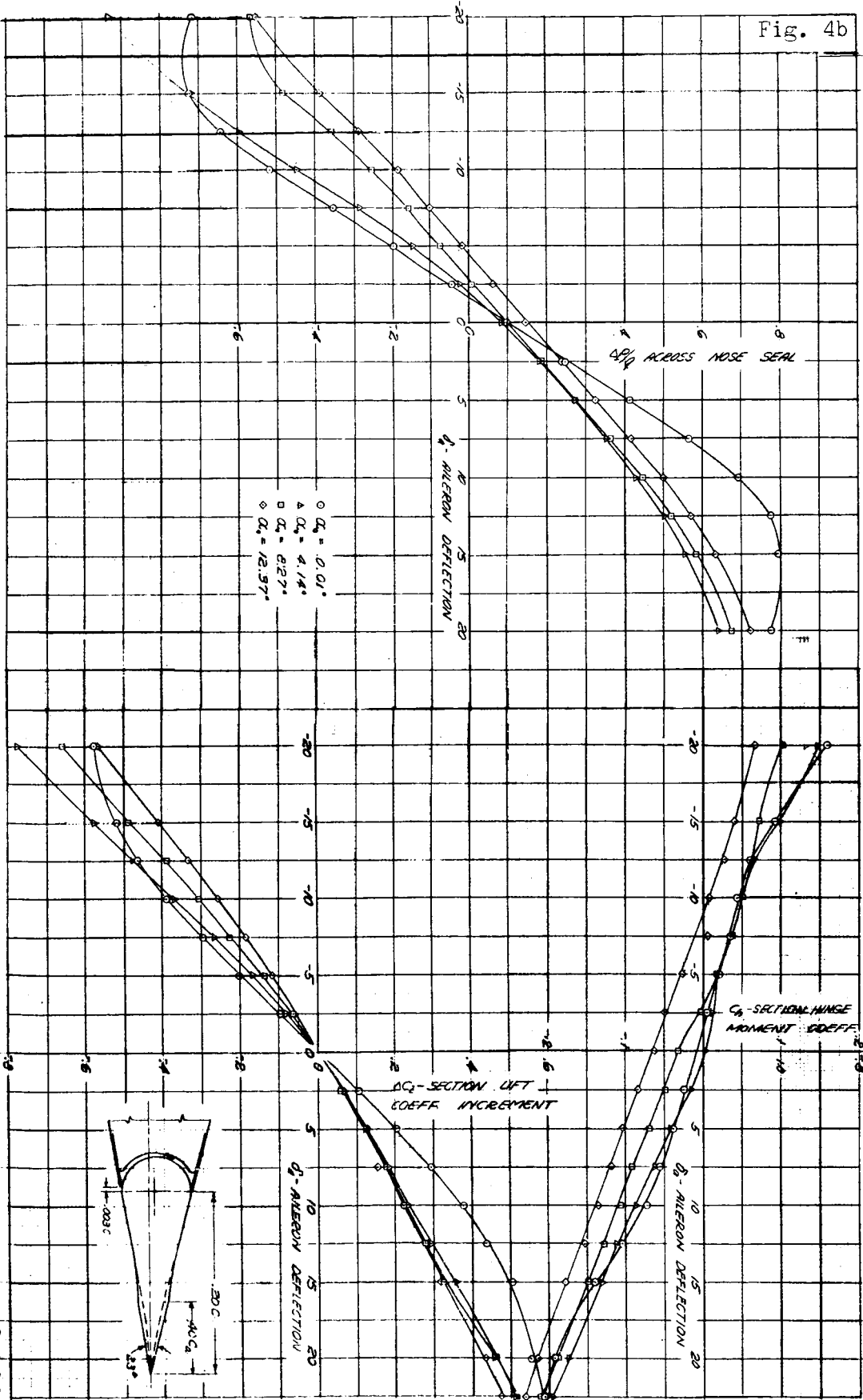


NACA

Fig. 4b

(1 block = 10/40")

FIGURE 4 - SECTION AERODYNAMIC CHARACTERISTICS OF AN NACA 0012 AIRFOIL STIMULATED WITH A 0.025-INCH SEALED SEALER, PRESSURE P = 30.135 PSF, R = 480,000



NACA

Fig. 5a

(1 block = 10/40")

FIGURE 5a - SECTION AERODYNAMIC CHARACTERISTICS OF AN NACA 00,2-215
($\alpha = 0.6$) AIRFOIL FORWARDED WITH A 0.20-CM-THICK SEALED GUM PLAIN
AILERON WITH A 0.30-G BEVELLED TRAILING EDGE
 $P = 180 \times 10^3$ PSF FT
 $R = 200,000$

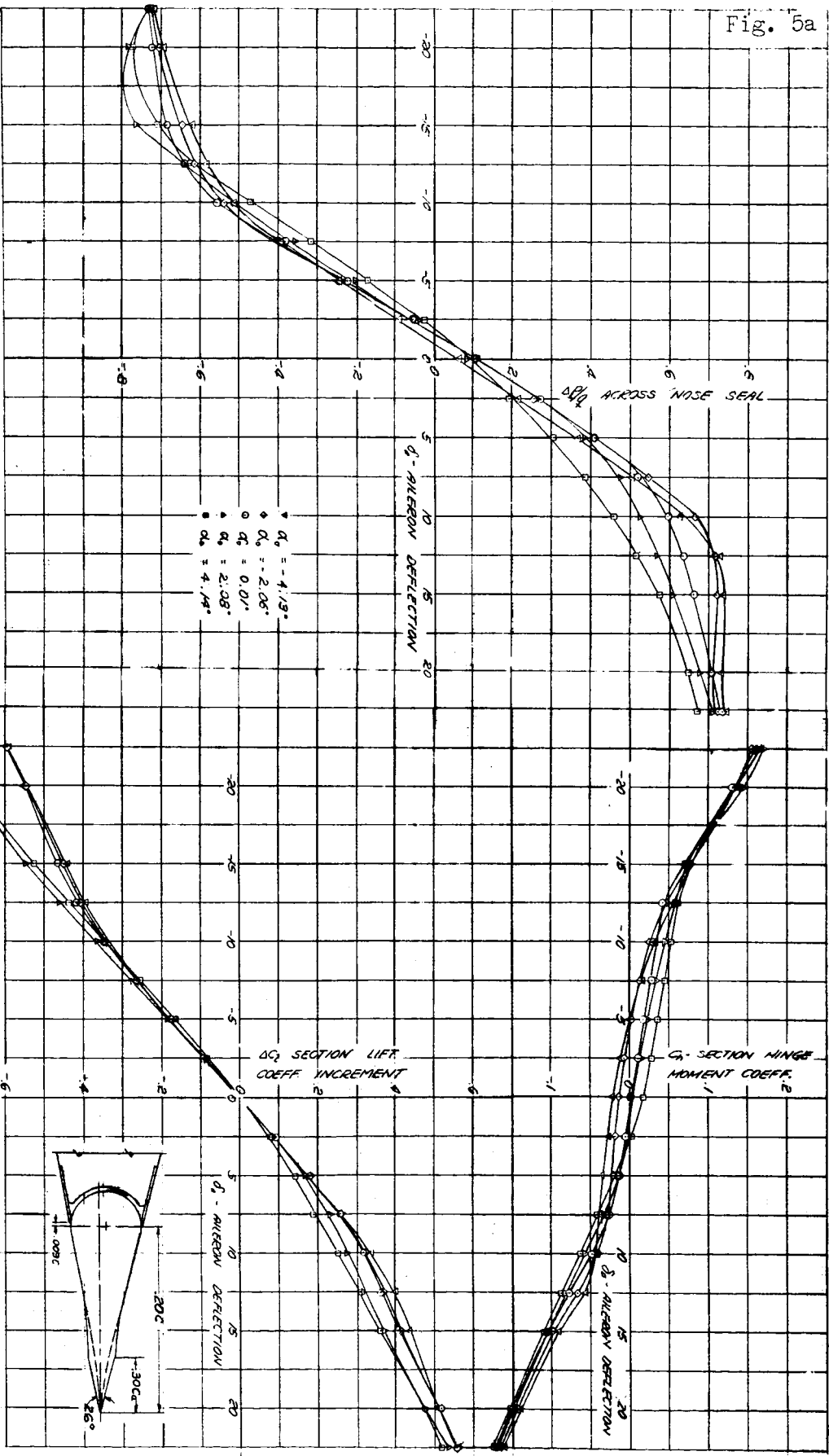
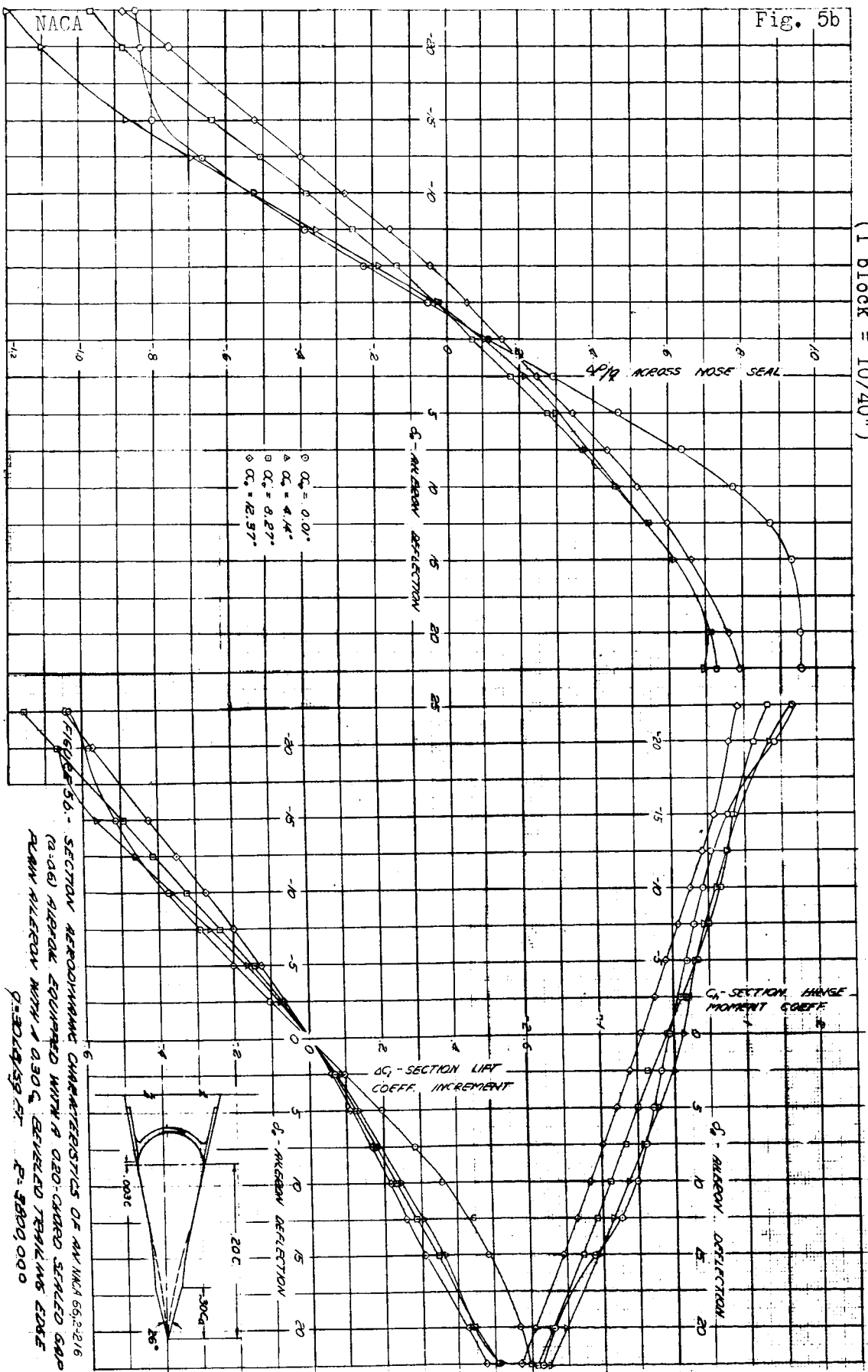


Fig. 5b

(1 block = 10/40")

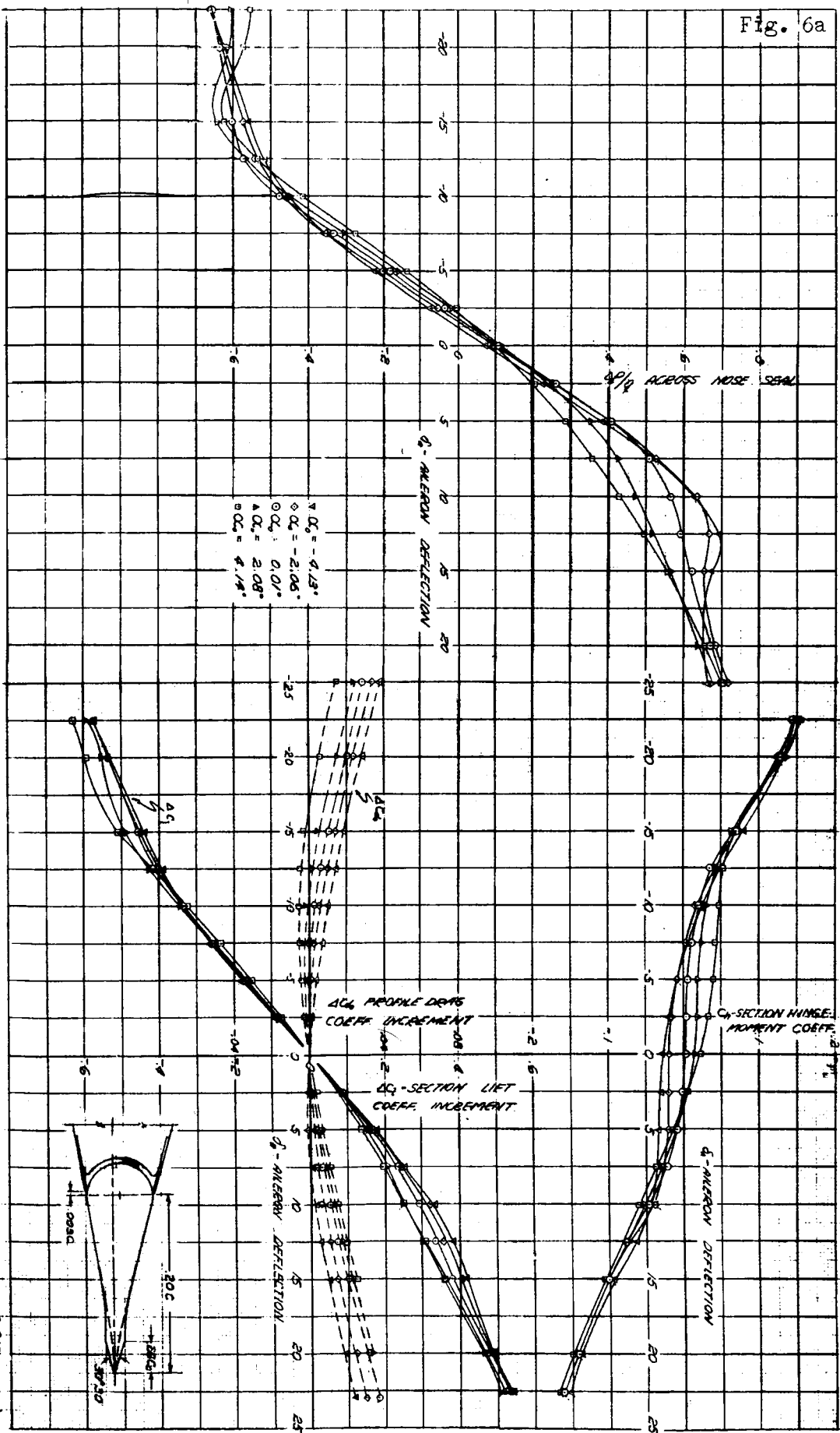


NACA

Fig. 6a

(1 block = 10/40")

FIGURE 6a - SECTION AERODYNAMIC CHARACTERISTICS OF AN AHEAD ASymmetrical RUBBER FENDERED WITH A 0.21 DEGREE STEELED ALUMINUM PLATE.
SECTION LENGTH = 0.20 C, CENTERED FORWARD OF THE STERN.

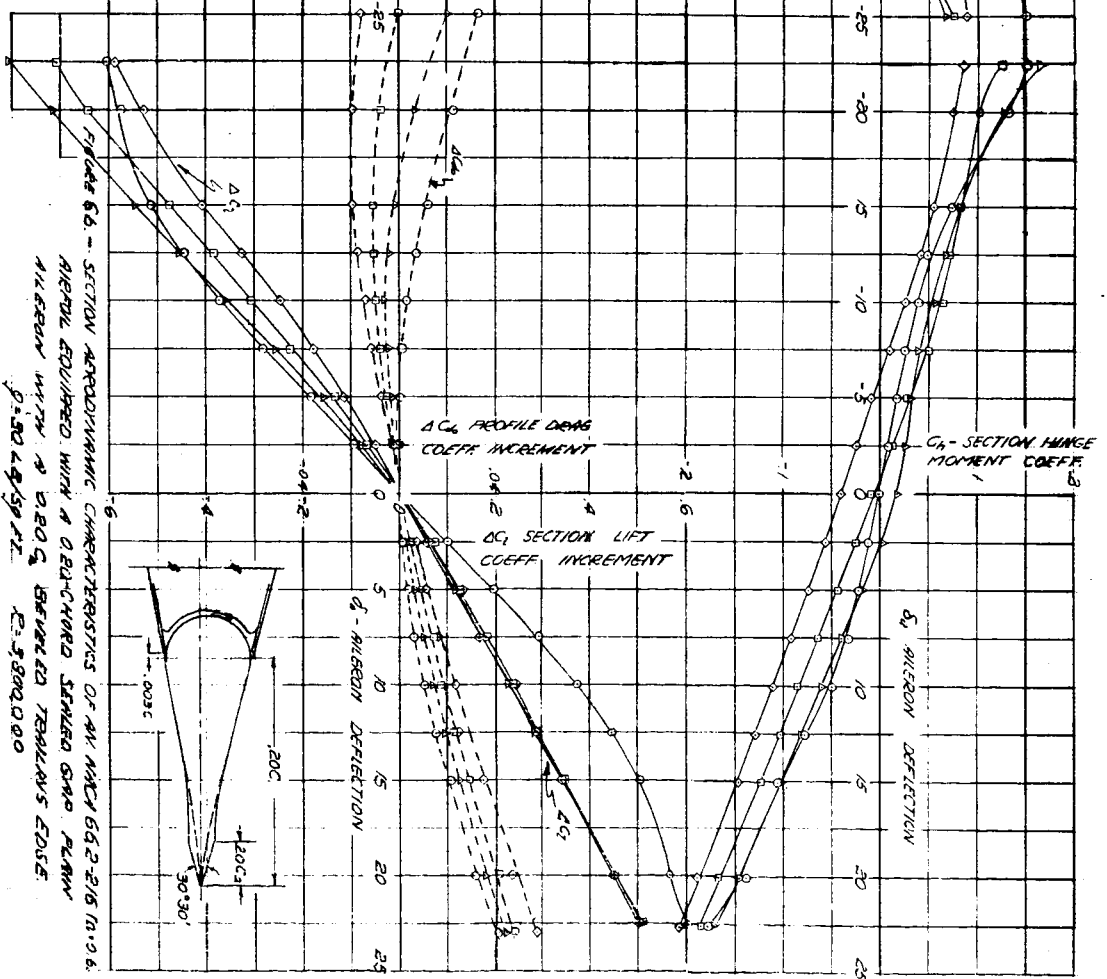


NACA

Fig. 6b

A-54

(1 block = 10/40")

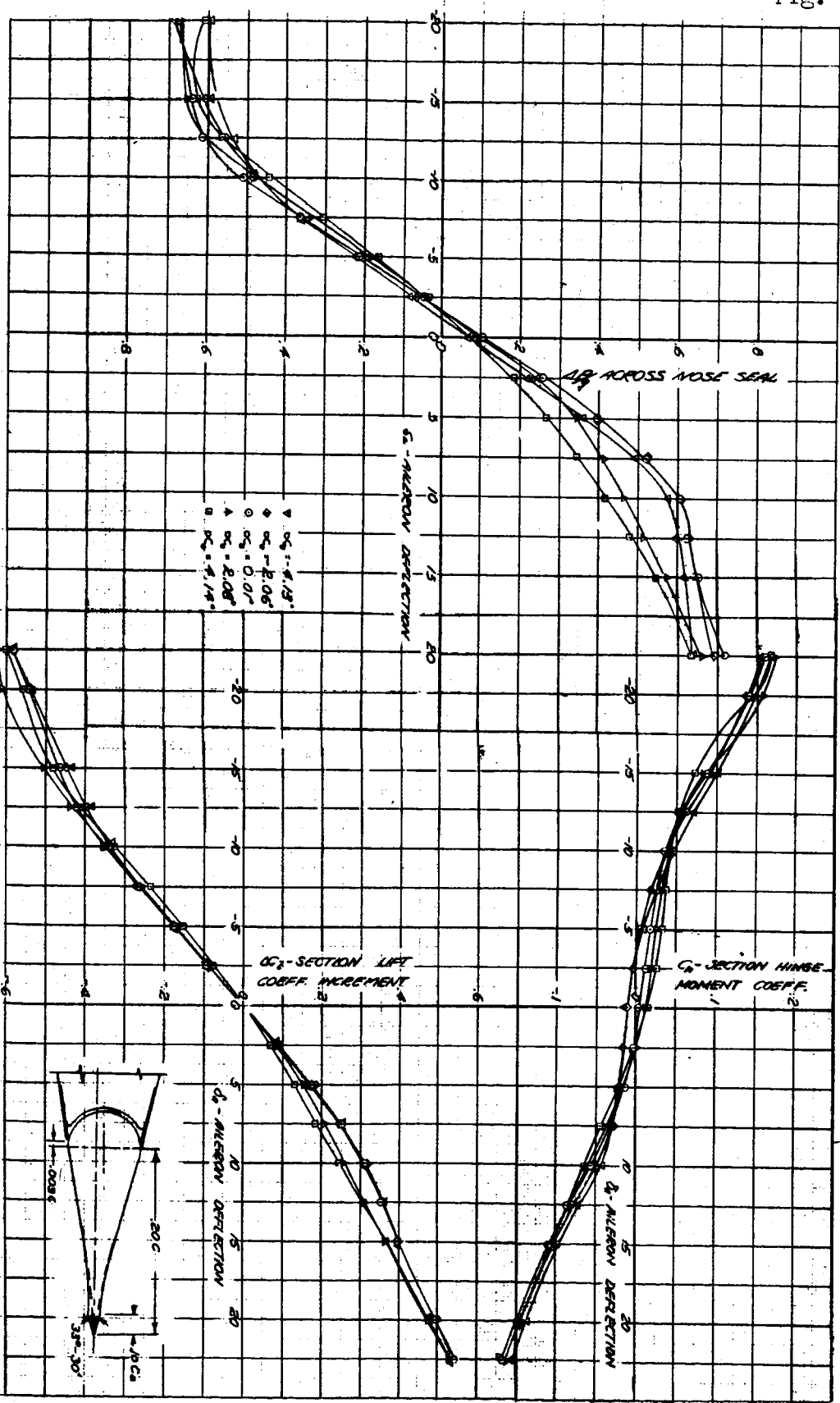


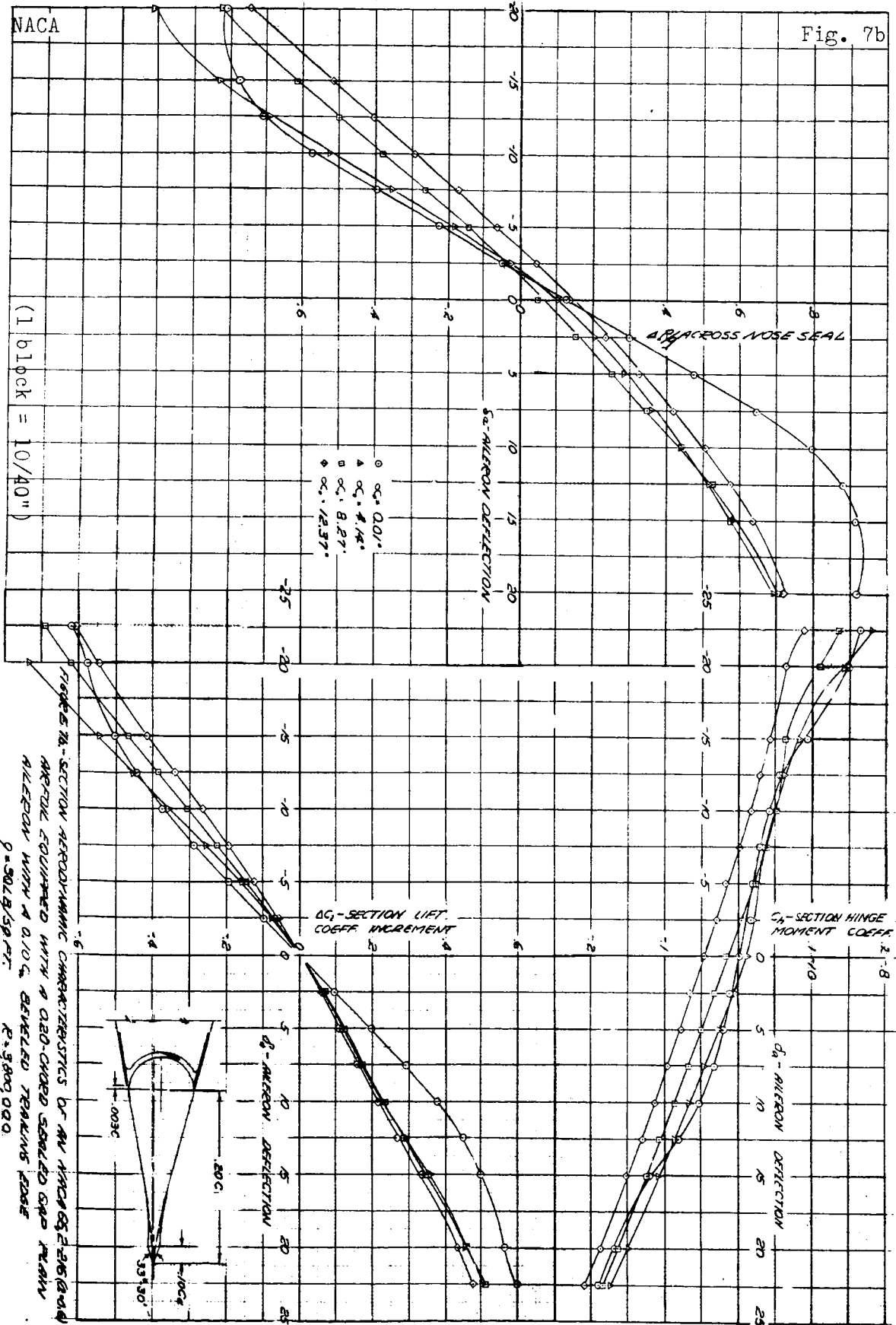
NACA

Fig. 7a

(1 block = 10/40")

FEARON - SECTION AERODYNAMIC CHARACTERISTICS OF AN NACA 652-215 (2.0-0.8)
AVERAGE COEFFICIENT NUMBER IN 12.0-CHINDED STAGGERED GRID
SECTION WITH 0.10% SURFACE TURBULENCE FLOOR
 $\rho = 100 \text{ kgm}^{-3}$ $V = 400 \text{ m/s}$





NACA

Fig. 8

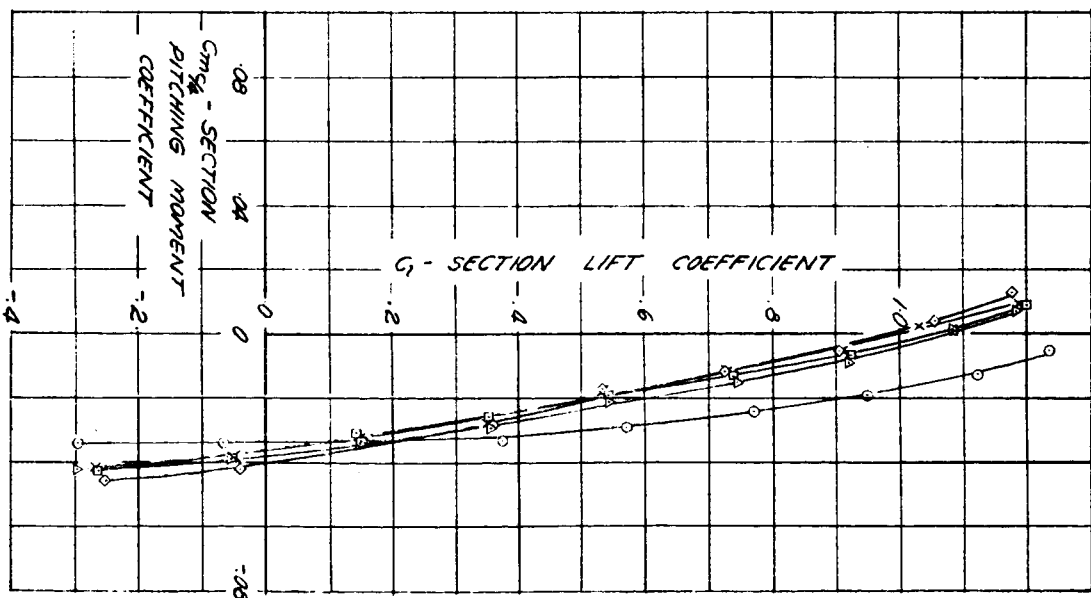
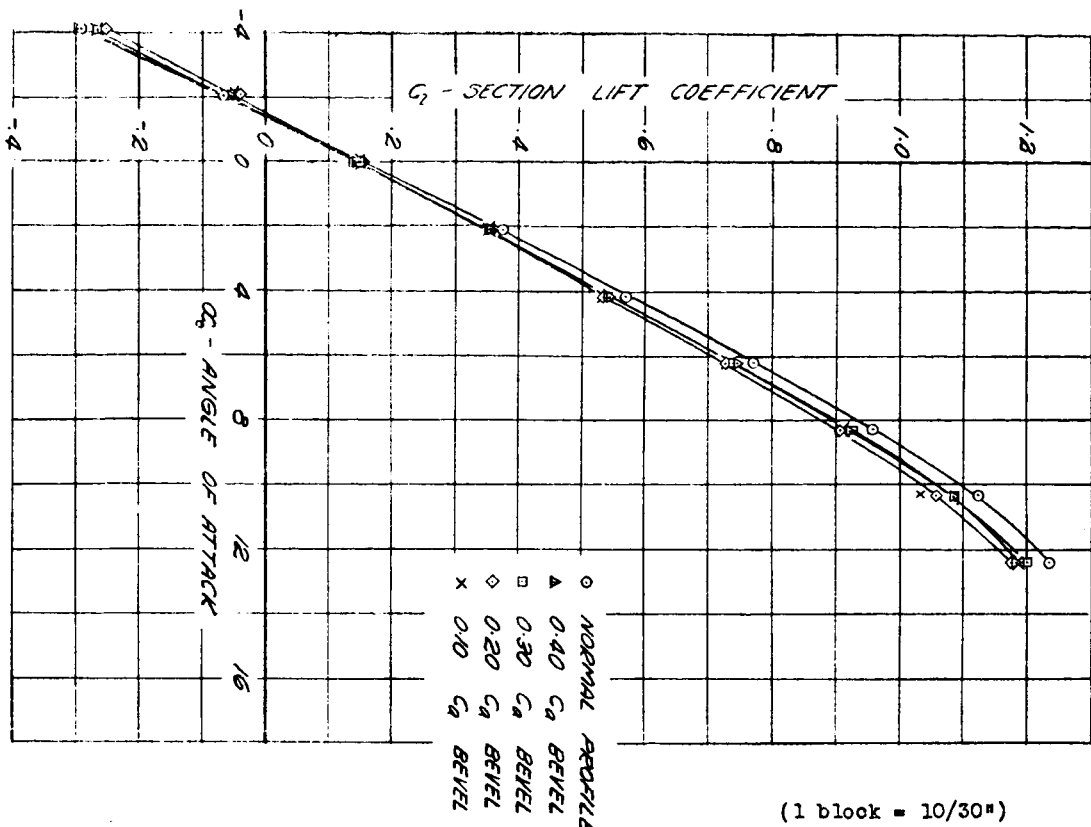
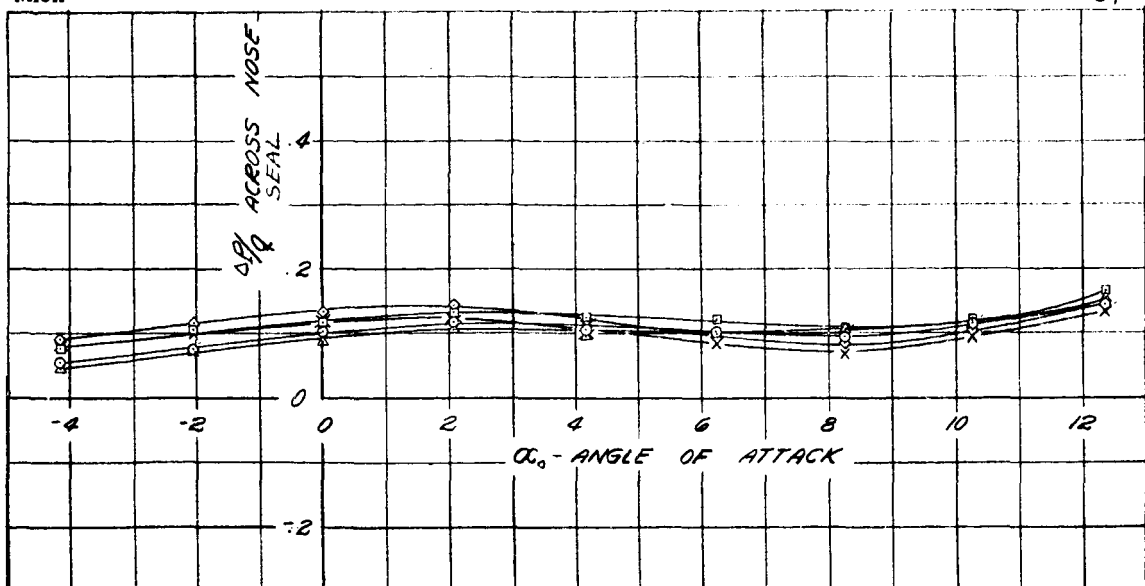


FIGURE 8 - EFFECT OF BEVELED TRAILING EDGE ON SECTION AERODYNAMIC CHARACTERISTICS OF AN NACA 66.2-216 ($\alpha = 0.6$) AIRFOIL EQUIPPED WITH A 0.20-CHORD SEALED GAP PLAIN AILERON. AILERON UNDEFLECTED
 $R = 8,200,000$



○ NORMAL PROFILE

△ 0.40 C_a BEVEL□ 0.30 C_a BEVEL◊ 0.20 C_a BEVEL× 0.10 C_a BEVEL

(1 block = 10/30°)

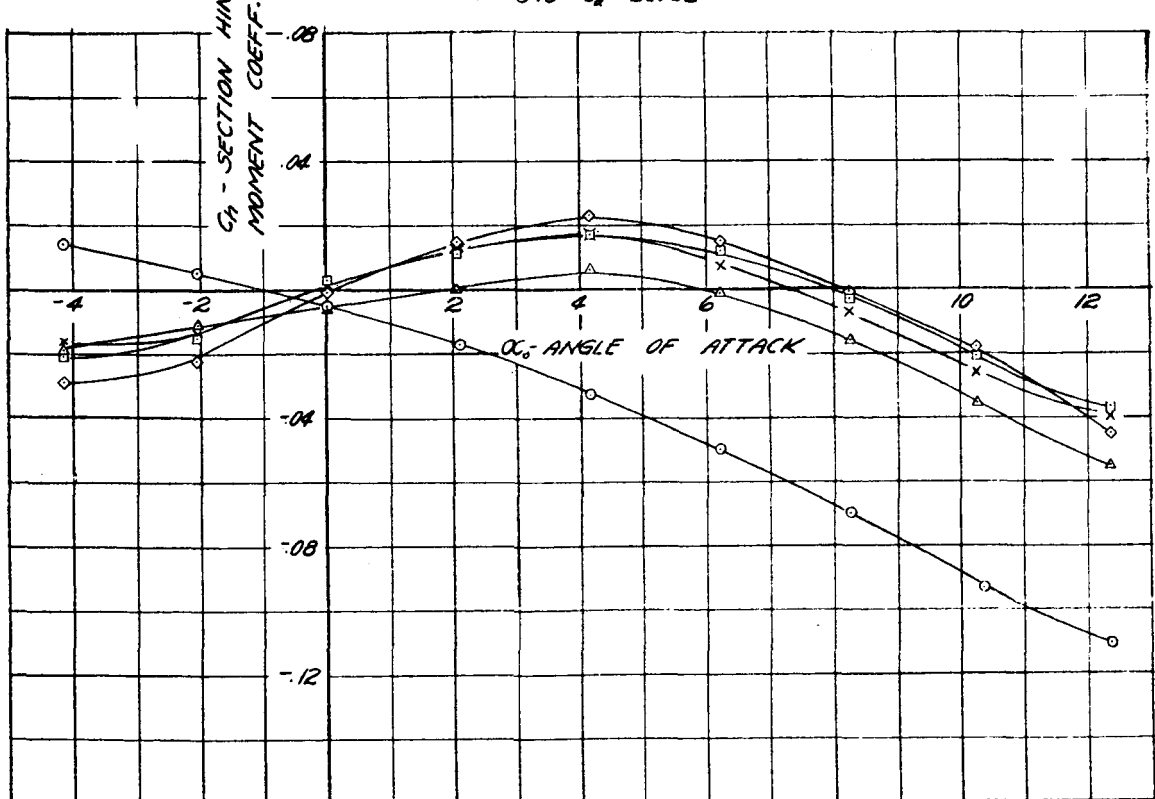
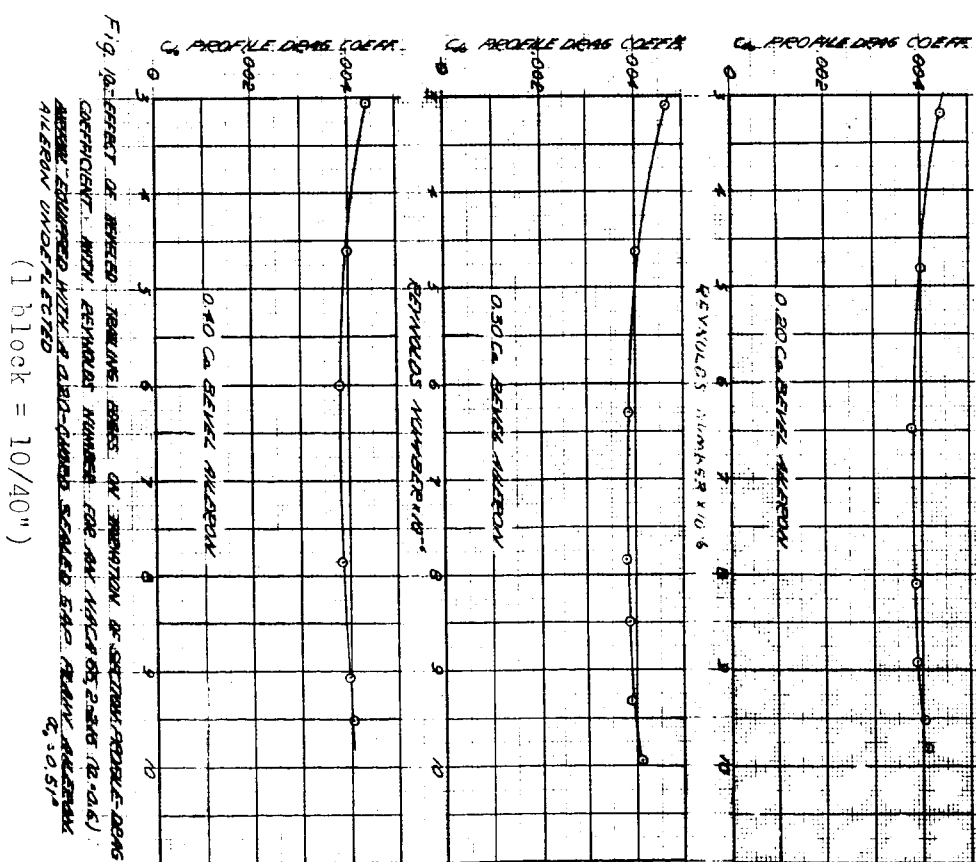
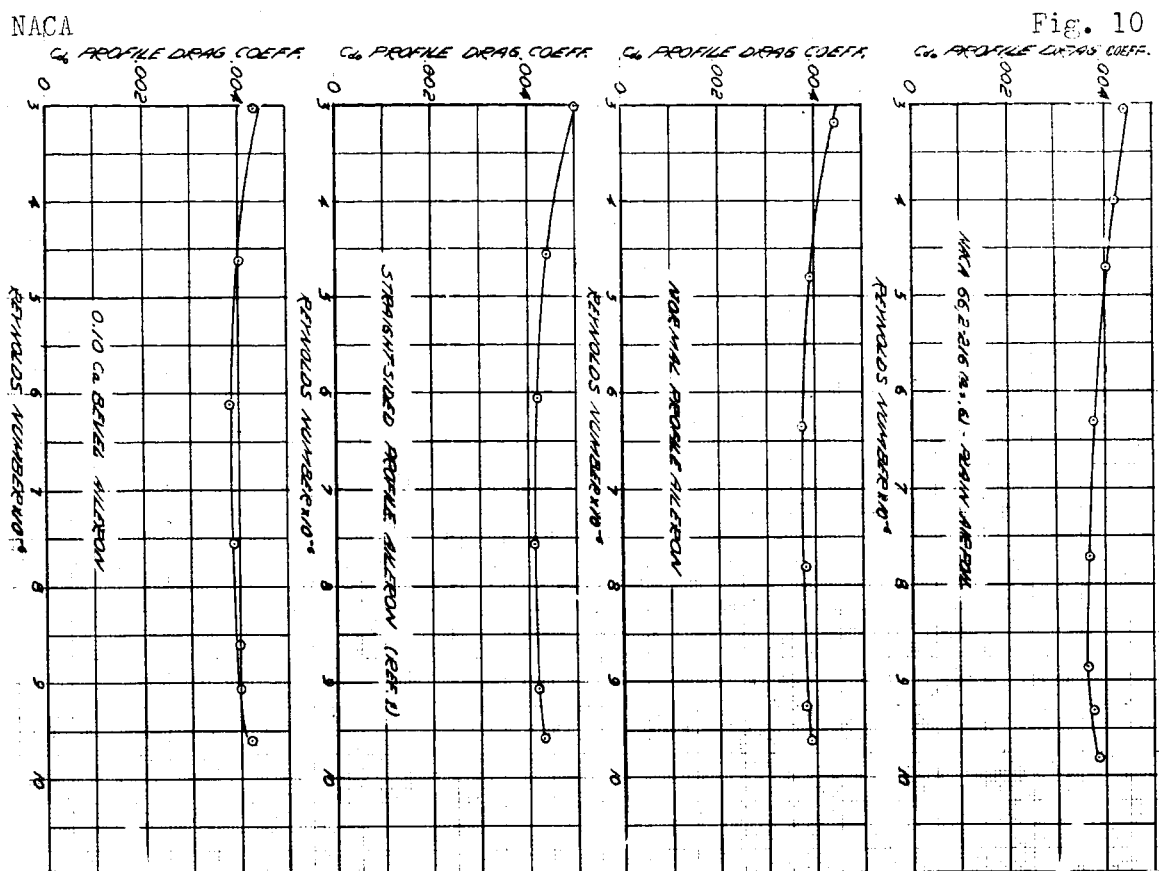


FIGURE 9.- EFFECT OF TRAILING EDGE BEVEL ON SECTION AERODYNAMIC CHARACTERISTICS OF AN NACA 66,2-216 ($\delta = 0.6$) AIRFOIL EQUIPPED WITH A 0.20-CHORD SEALED GAP PLAIN AILERON AILERON UNDEFLECTED $R=8200,000$

Fig. 10



NACA

Fig. 11

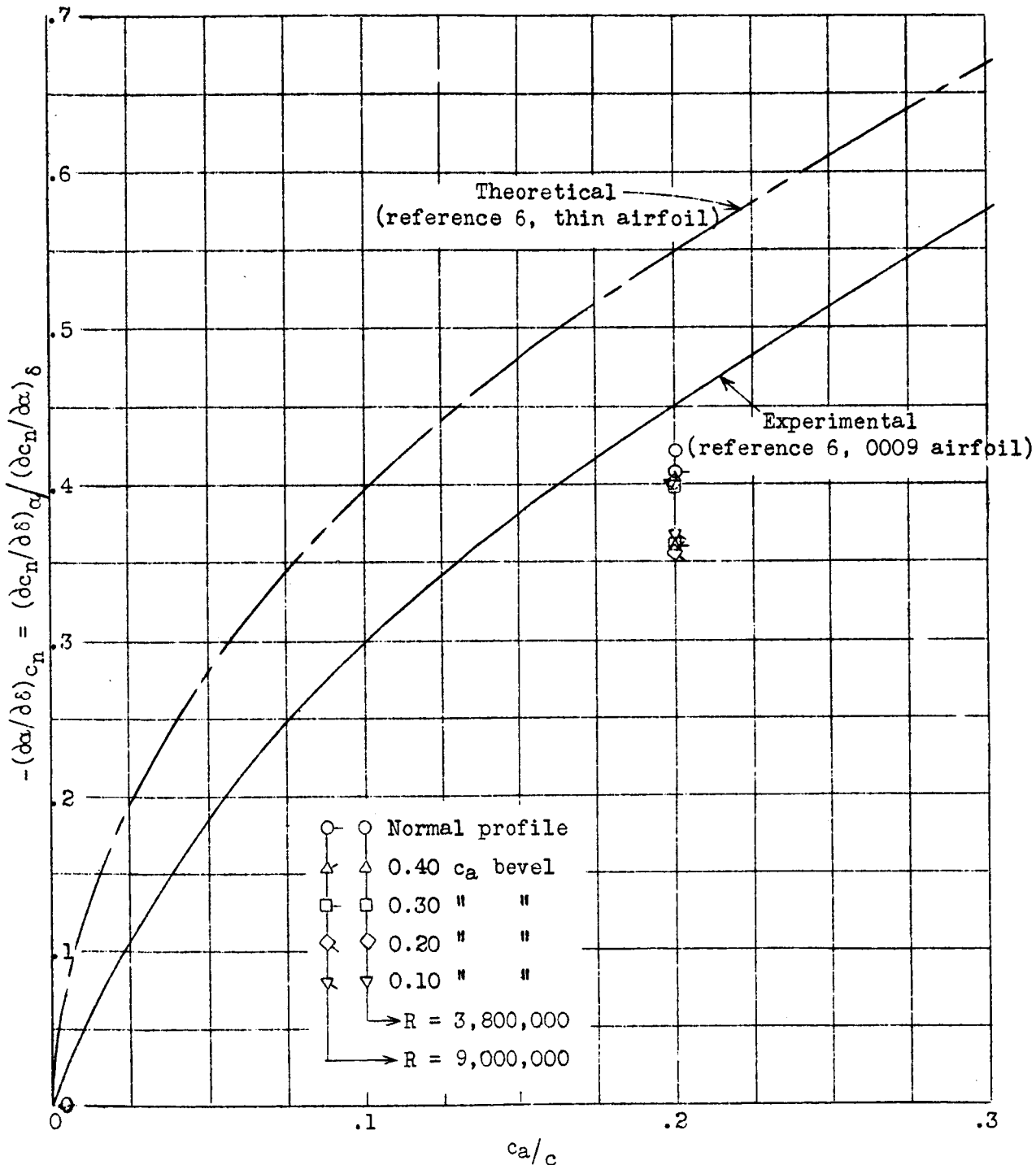


Figure 11.- Effect of beveled trailing edge ailerons on the aileron effectiveness parameter for sealed gap ailerons of 0.20-chord on an NACA 66,2-216 ($a = 0.6$) airfoil.

NACA

Fig. 12

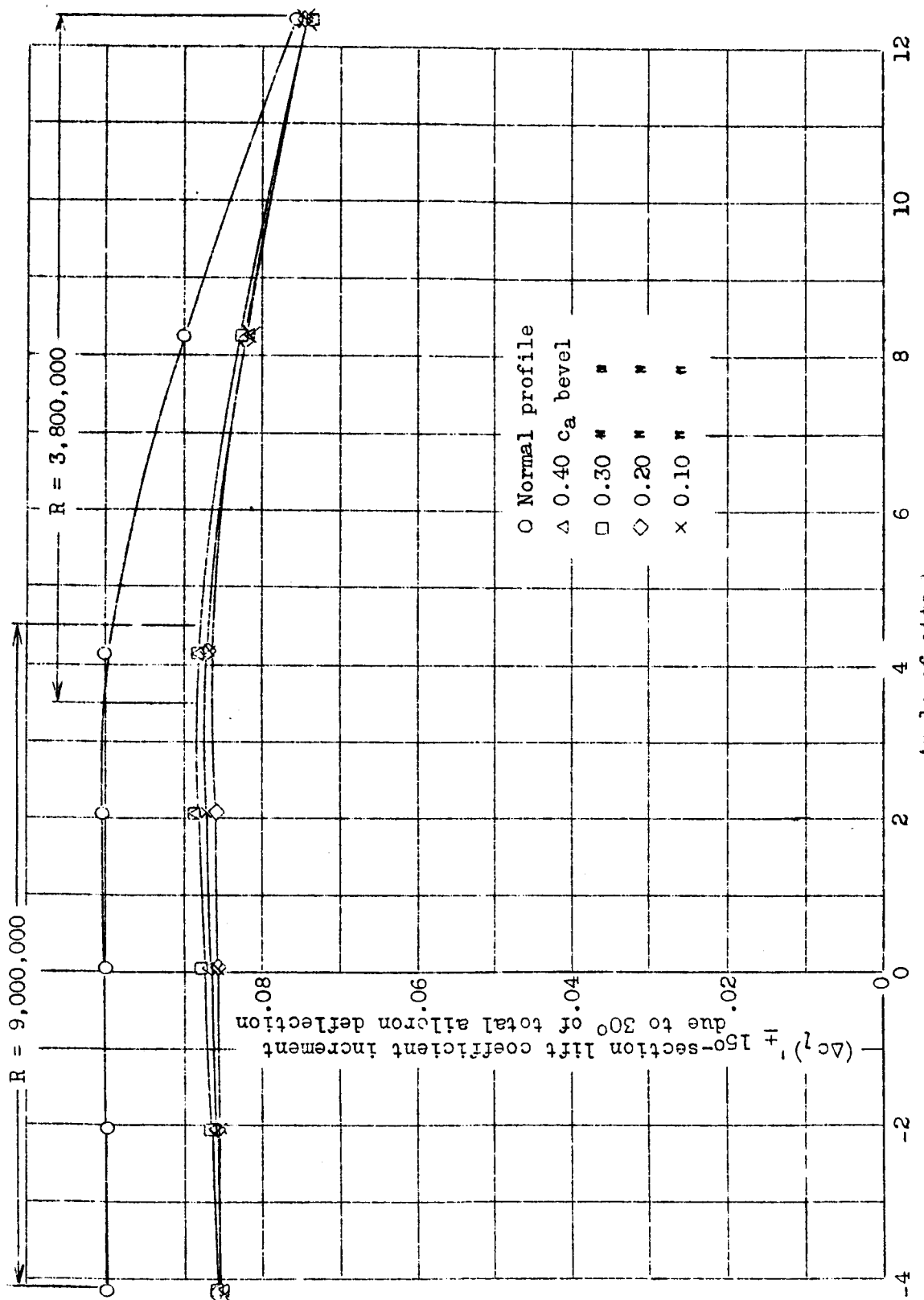


Figure 12.—Effect of beveled trailing edges on aileron effectiveness for an NACA 66,2-216 ($a = 0.6$) airfoil equipped with sealed gap plain ailerons of 0.20 chord.

Fig. 13

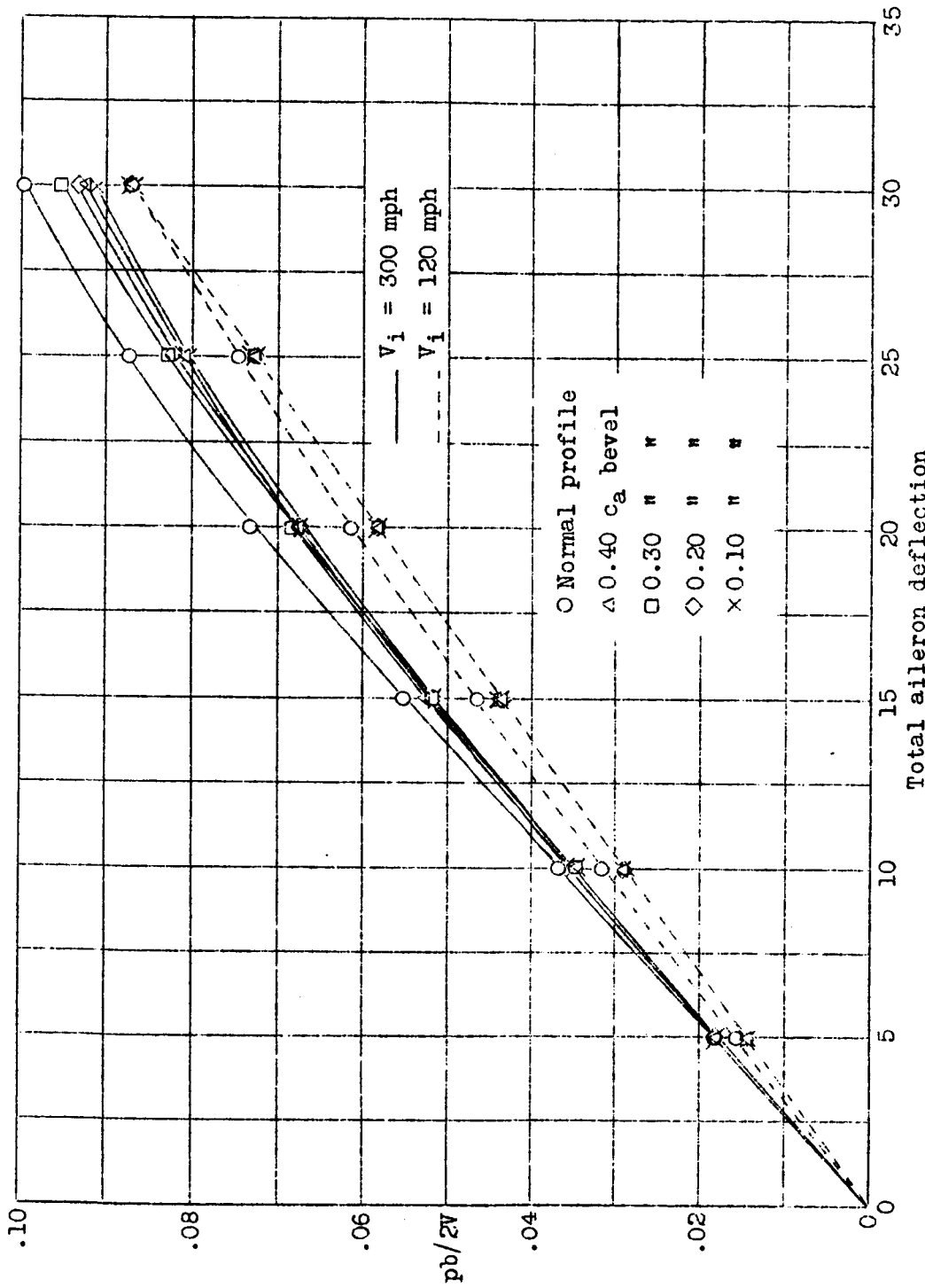


Figure 13.- Effect of beveled trailing edge on aileron effectiveness as applied to a typical pursuit airplane; 0.20-chord sealed gap ailerons equal up and down aileron deflection; assumed rigid wing and zero sideslip.

NACA

Fig. 14

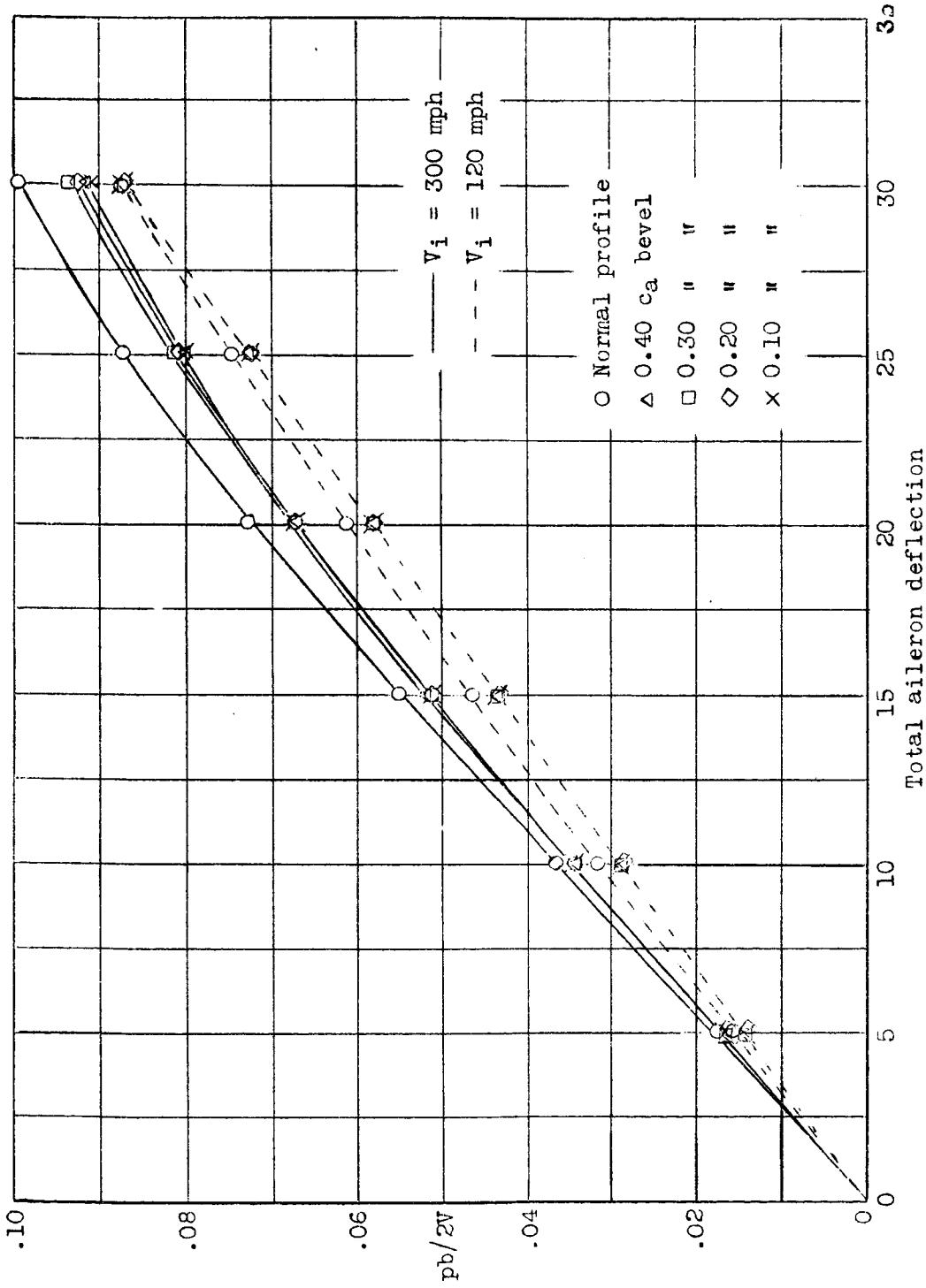


Figure 14.- Effect of beveled trailing edges on aeron effectiveness as applied to a typical medium bomber; 0.20-chord sealed gap ailerons; equal up and down aileron deflection; assumed rigid wing and zero sideslip.

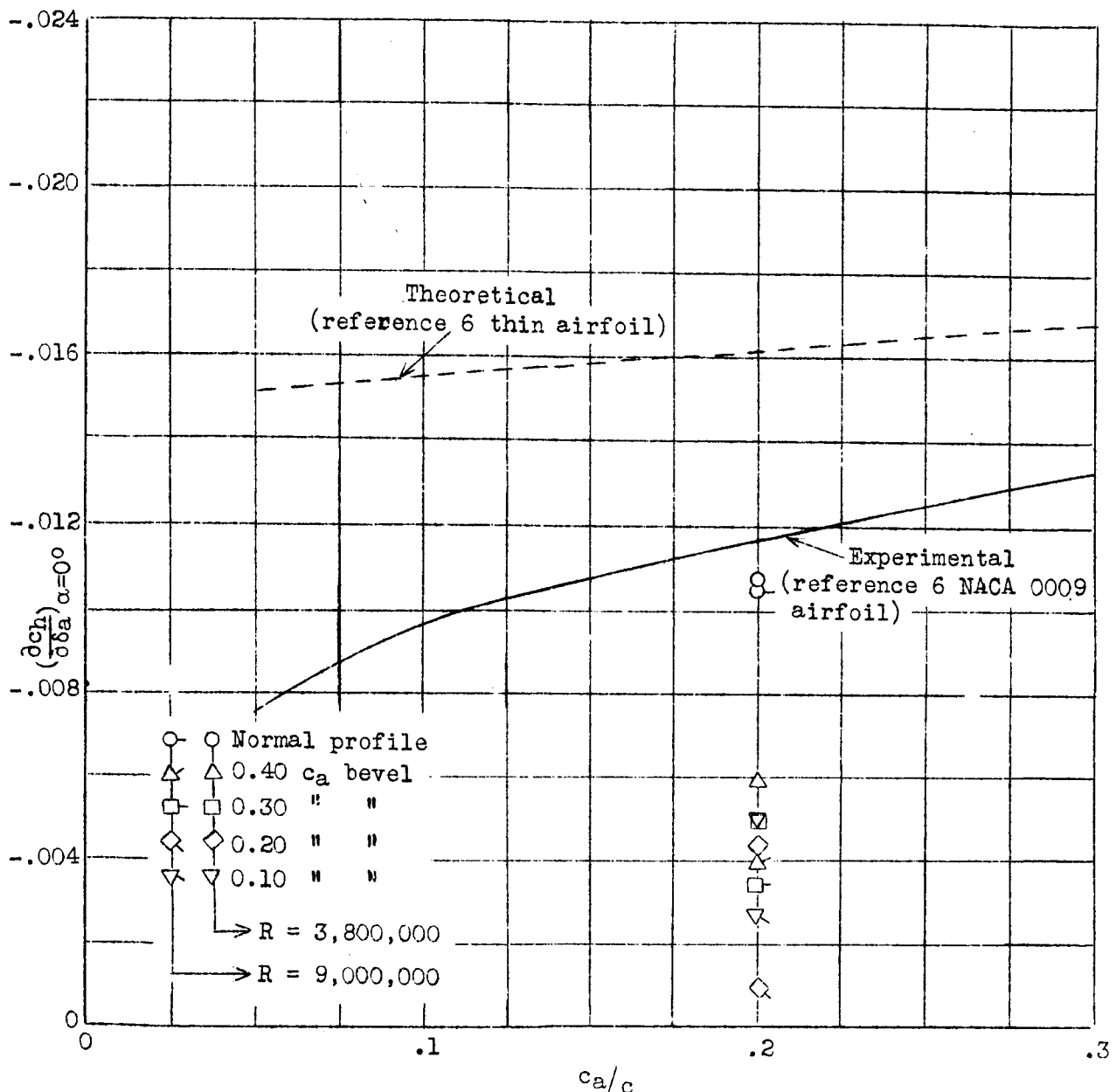


Figure 15.- Effect of beveled trailing edge ailerons on the aileron hinge moment parameter for sealed gap plain ailerons of 0.20 chord on an NACA 66,2-216 ($a = 0.6$) airfoil.

NACA

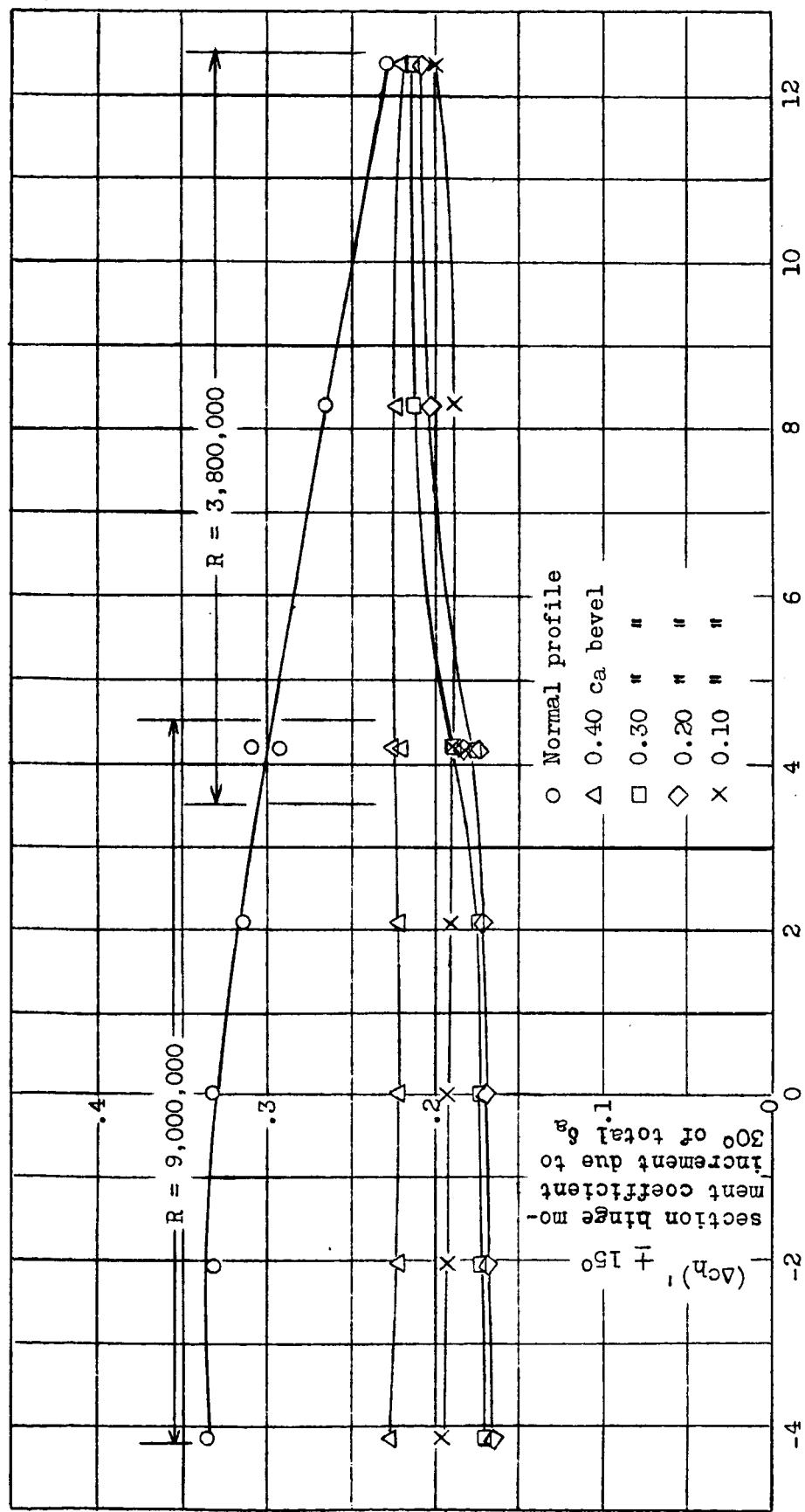
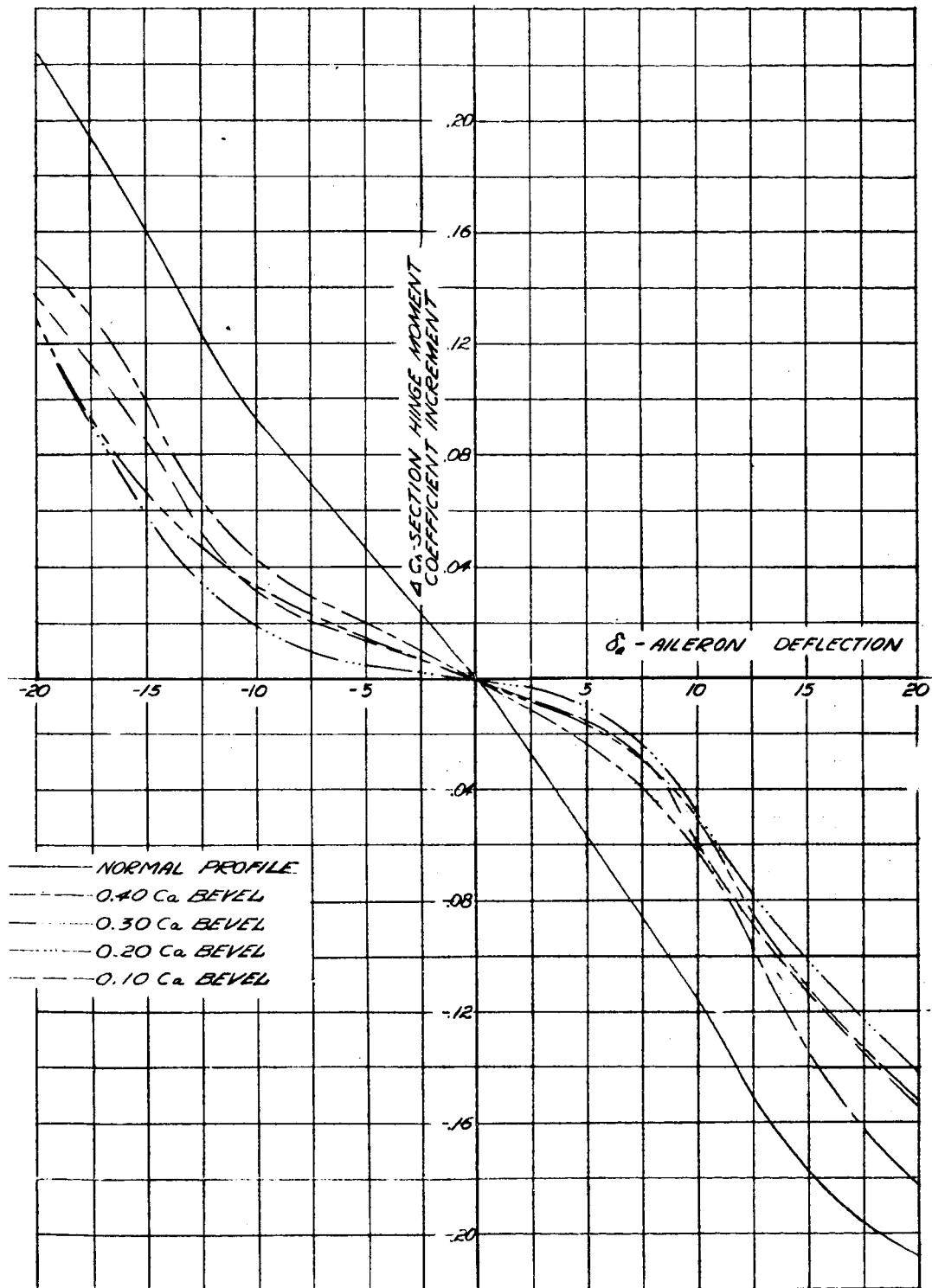


Fig. 16

Figure 16.— Effect of beveled trailing edges on aileron hinge moments for an NACA 66,2-216 ($a = 0.6$) airfoil equipped with sealed gap plain ailerons of 0.20 chord.

A-54



(1 block = 10/30")

FIG. 17.- EFFECT OF BEVELED TRAILING EDGES ON ΔC_h VS. δ_a FOR 0.20-CHORD SEALED GAP PLAIN AILERONS ON AN NACA 66,2-216 ($\alpha=0.6$) AIRFOIL.
 $Q = 180 \text{ LB/SQ. FT.}$ $R = 9,000,000$

NACA

Fig. 18

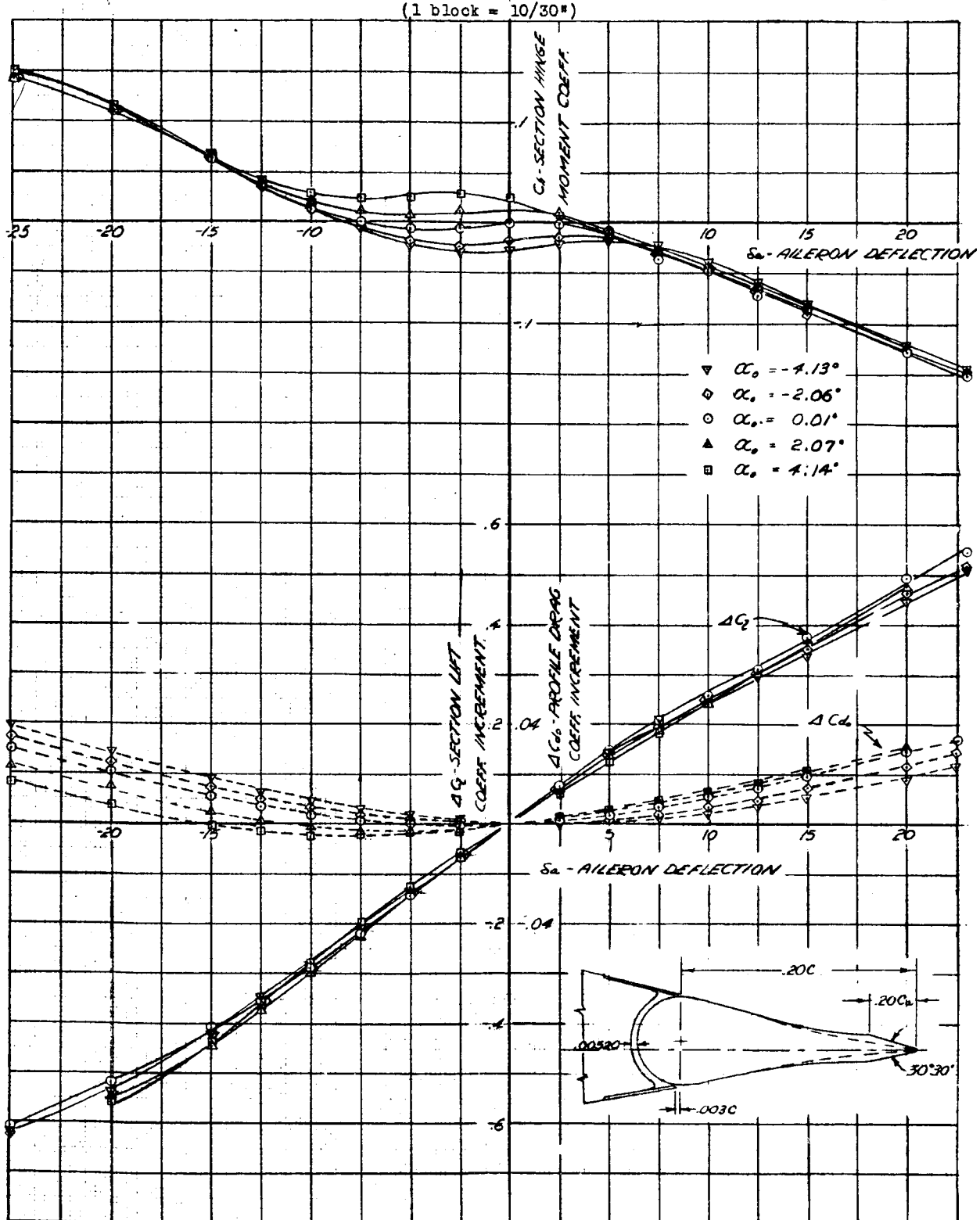


FIGURE 18. - SECTION AERODYNAMIC CHARACTERISTICS OF AN NACA 66,2-216 (C_D=0.6) AIRFOIL EQUIPPED WITH A 0.20-CHORD PLAIN AILERON WITH A 0.20 C BEVELED TRAILING EDGE AND 0.05 C NOSE GAP
 $R=9,000,000$

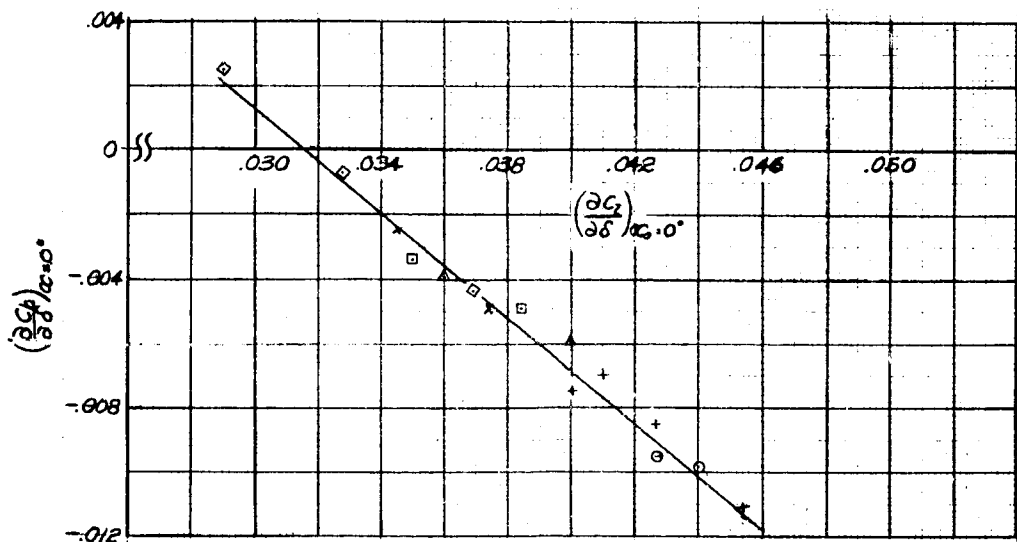
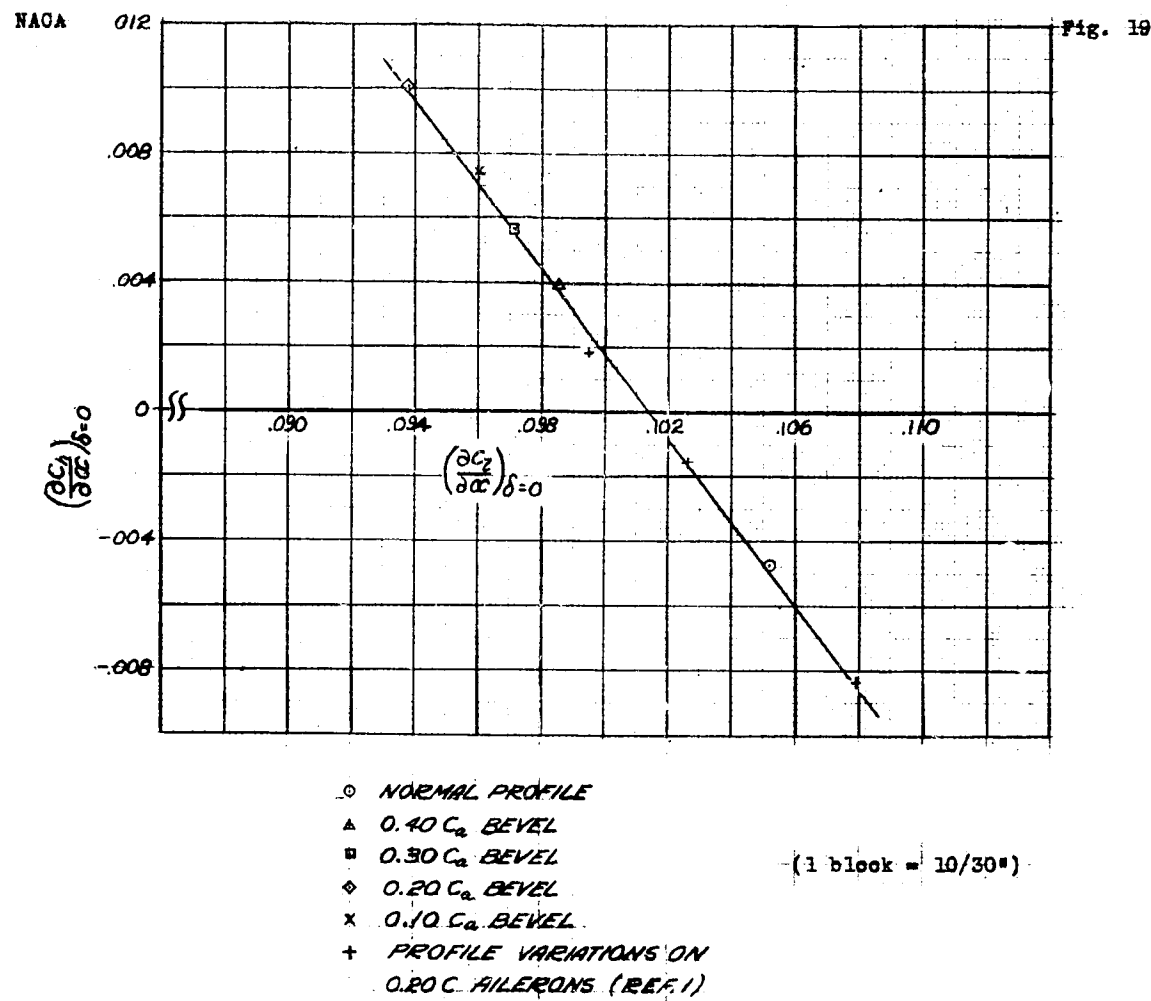
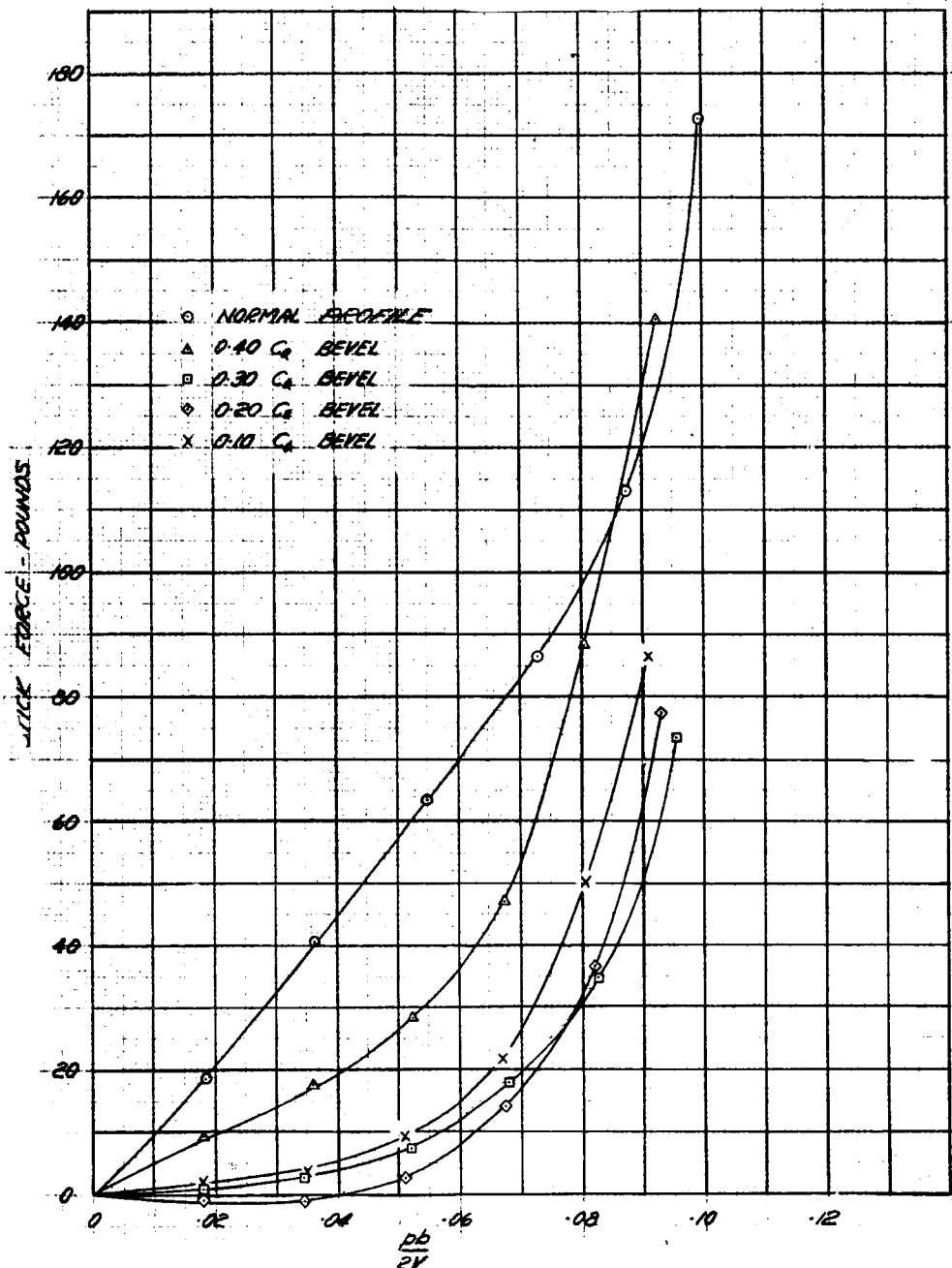


FIGURE 19. - VARIATION OF HINGE MOMENT PARAMETERS WITH LIFT PARAMETERS FOR AN NACA 66,2-216 ($\alpha = 0.6$) AIRFOIL EQUIPPED WITH A 0.20 CHORD SEALED GAP PLAIN AILERON.



(1 block = 10/30°)

FIGURE 20.—EFFECT OF BEVELED TRAILING EDGES ON THE AILERON-CONTROL CHARACTERISTICS OF A TYPICAL PURSUIT AIRPLANE EQUIPPED WITH 0.20-CHORD SEALED GAP AILERONS WITH 0.40 C_g INTERNAL NOSE BALANCE AT AN INDICATED AIRSPEED OF 300 MPH.

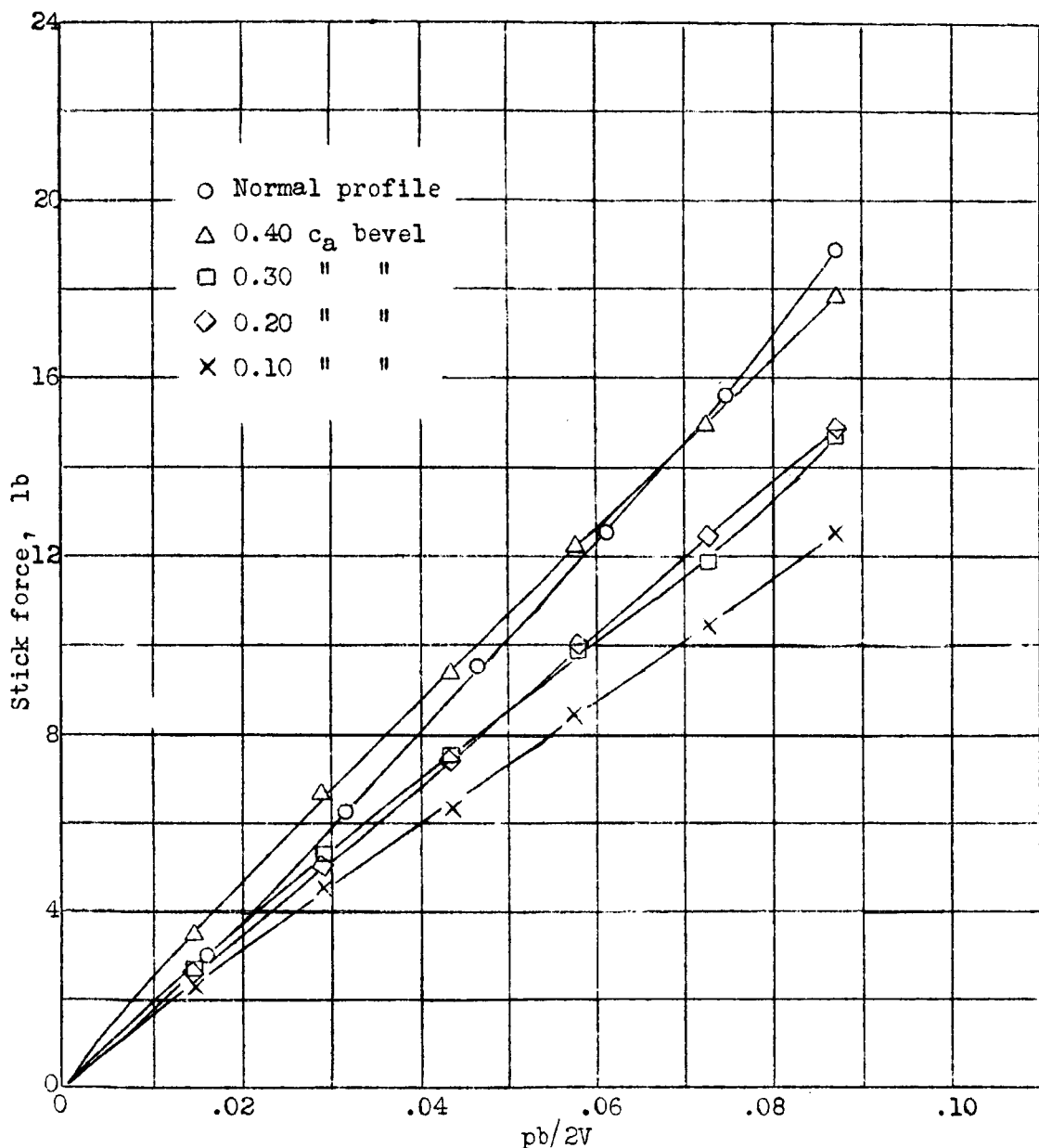


Figure 21.- Effect of beveled trailing edges on the aileron-control characteristics of a typical pursuit airplane equipped with 0.20-chord sealed gap ailerons with $0.40 c_a$ internal nose balance at an indicated airspeed of 120 mph.

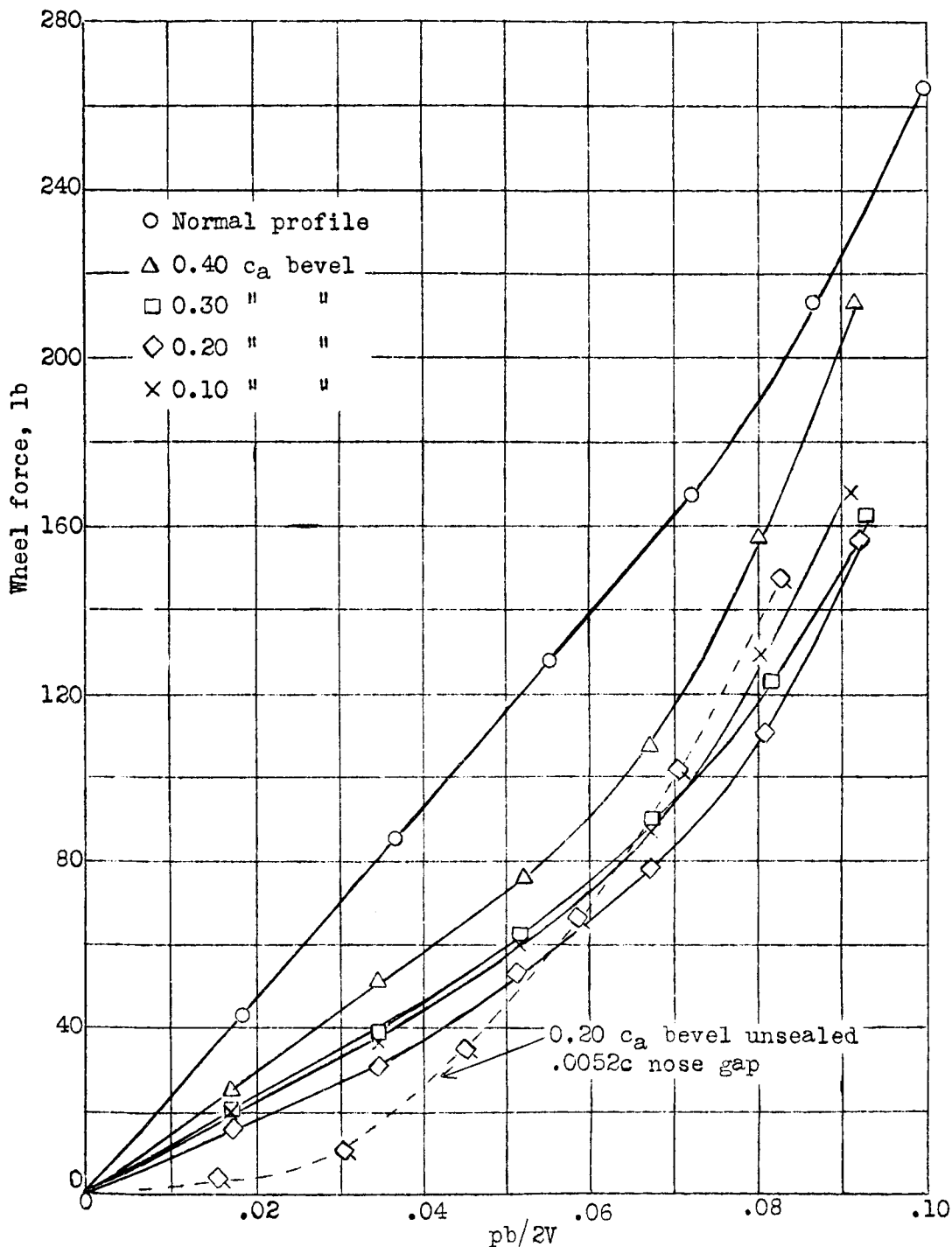


Figure 22.— Effect of beveled trailing edges on the aileron-control characteristics of a medium bomber equipped with 0.20-chord sealed gap ailerons with no nose balance at an indicated airspeed of 250 mph.

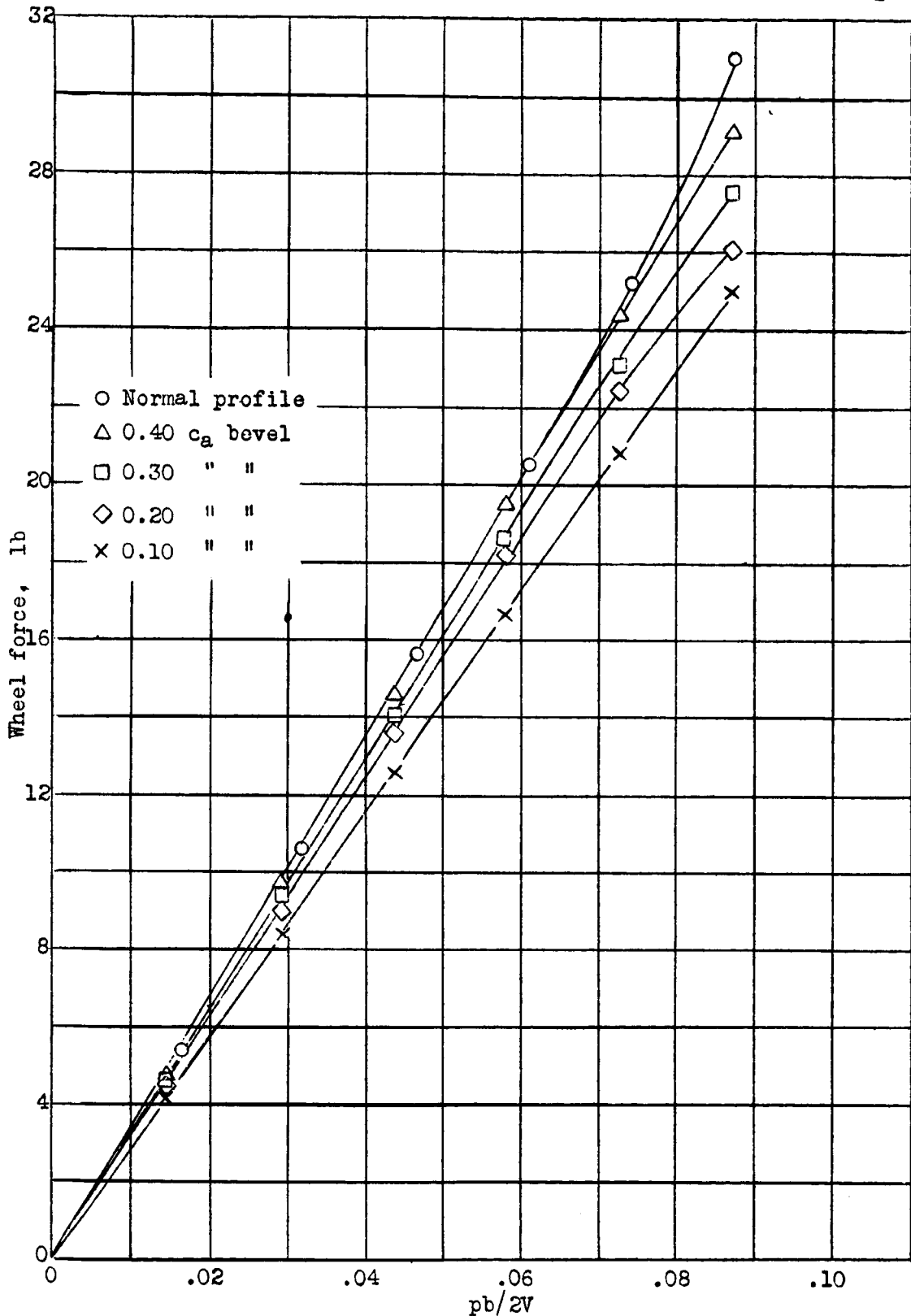


Figure 23.— Effect of beveled trailing edges on the aileron-control characteristics of a medium bomber equipped with 0.20-chord sealed gap ailerons with no nose balance at an indicated airspeed of 250 mph.

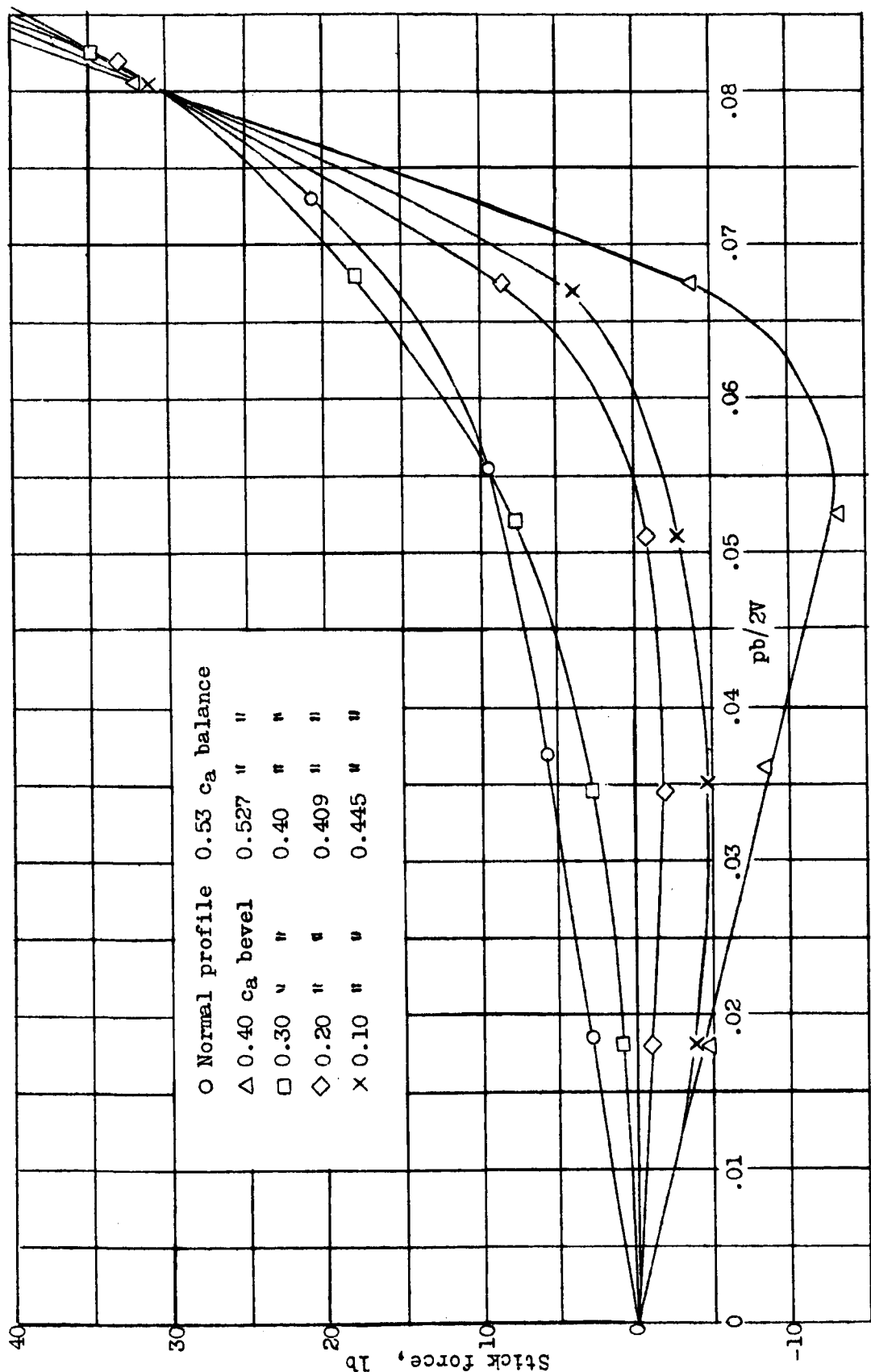


Figure 24.—Effect of beveled trailing edges on the aileron-control characteristics of a typical pursuit airplane equipped with 0.20-chord sealed gap ailerons with sufficient internal nose balance for a 30-pound high-speed stick force at a $p_b/2V$ of 0.08. $V_1 = 300$ mph.

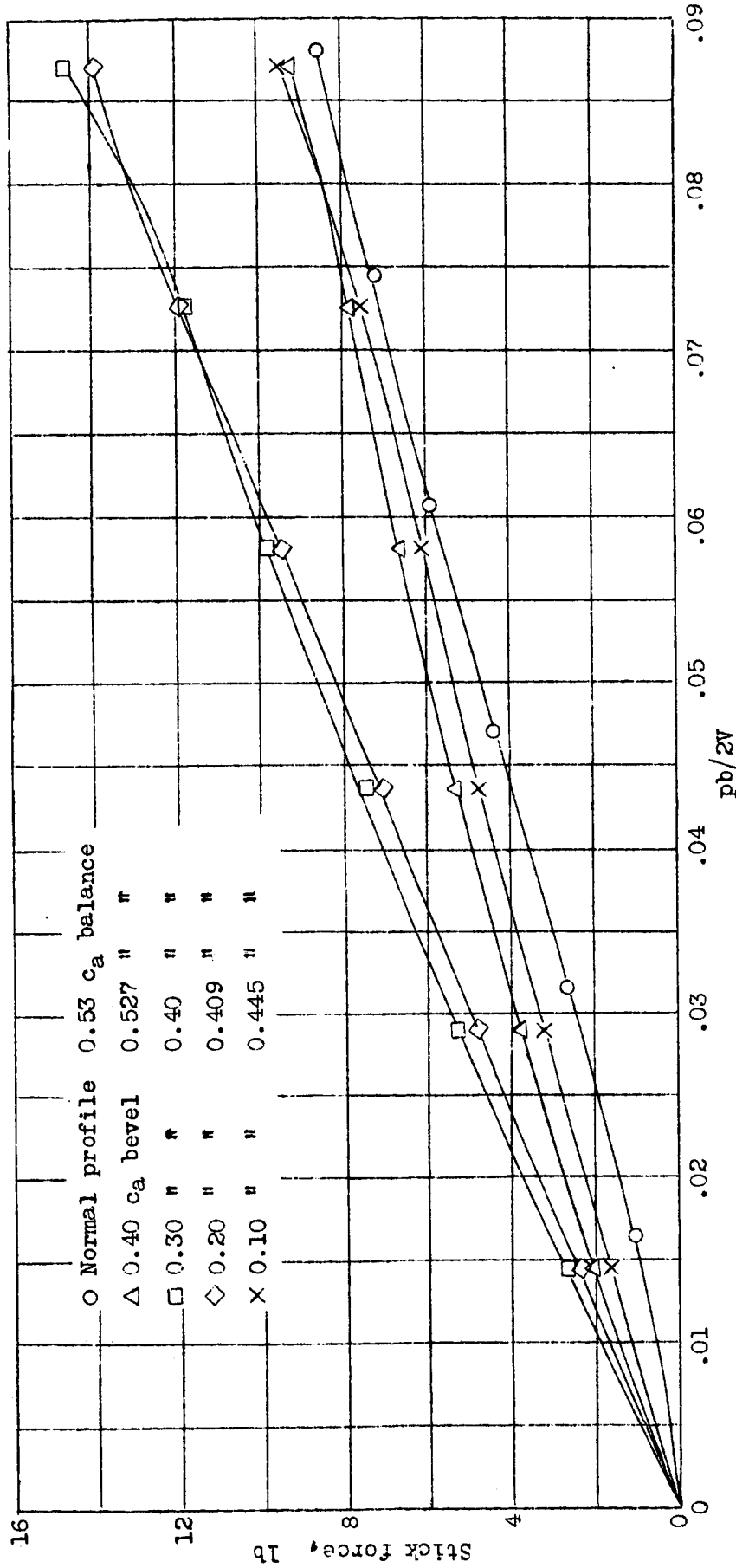


Figure 25.— Effect of beveled trailing edges on the aileron-control characteristics of a typical pursuit airplane equipped with 0.20-chord sealed gap ailerons with sufficient internal nose balance for a 30-pound high-speed stick force at a $pb/2V$ of 0.08. $V_1 = 120$ mph.

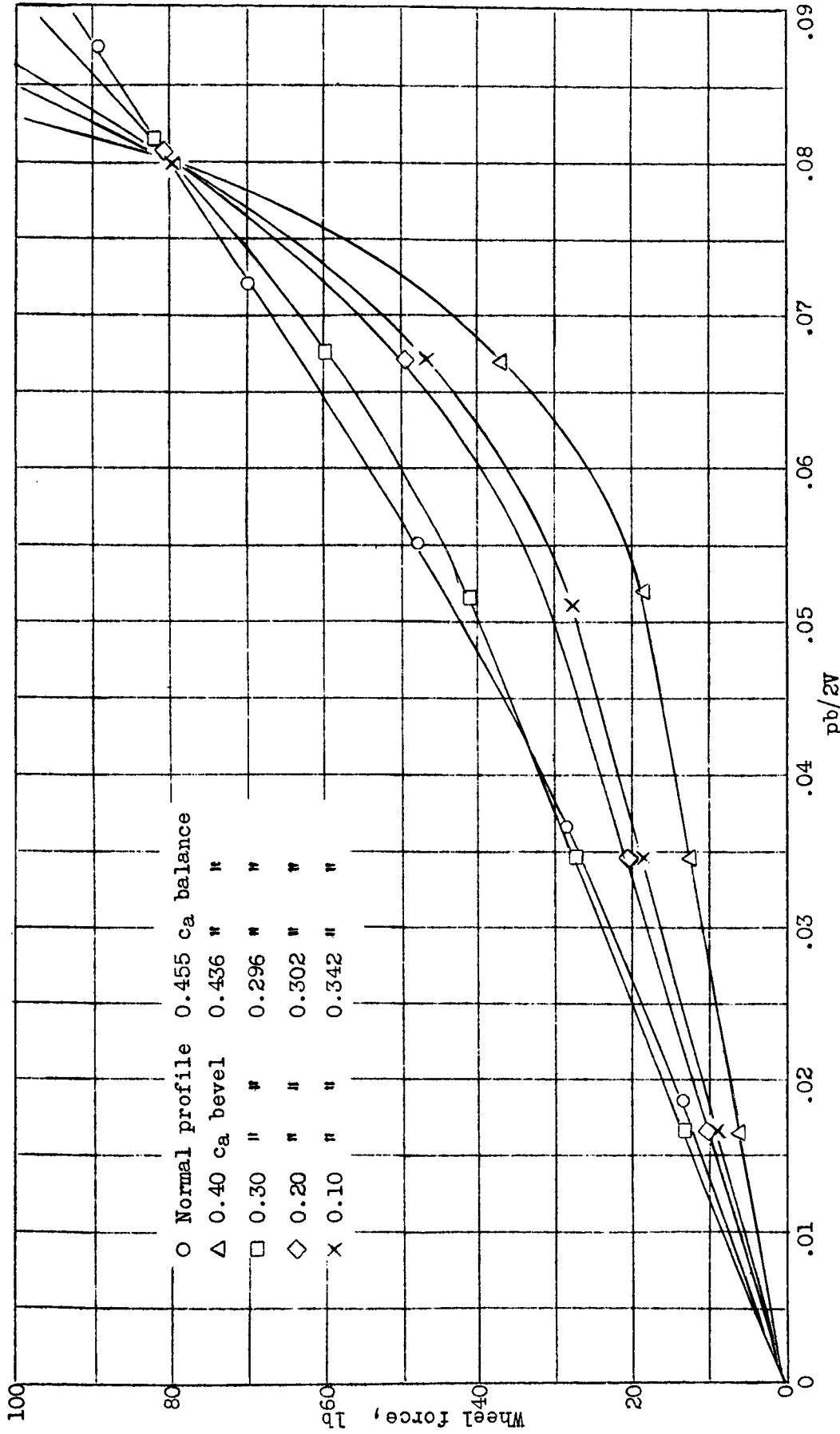


Figure 26.—Effect of beveled trailing edges on the aileron-control characteristics of a typical medium bomber equipped with 0.20-chord sealed gap ailerons with sufficient internal nose balance for a 80-pound high-speed wheel force at a $pb/2V$ of 0.08. $V_1 = 250$ mph.

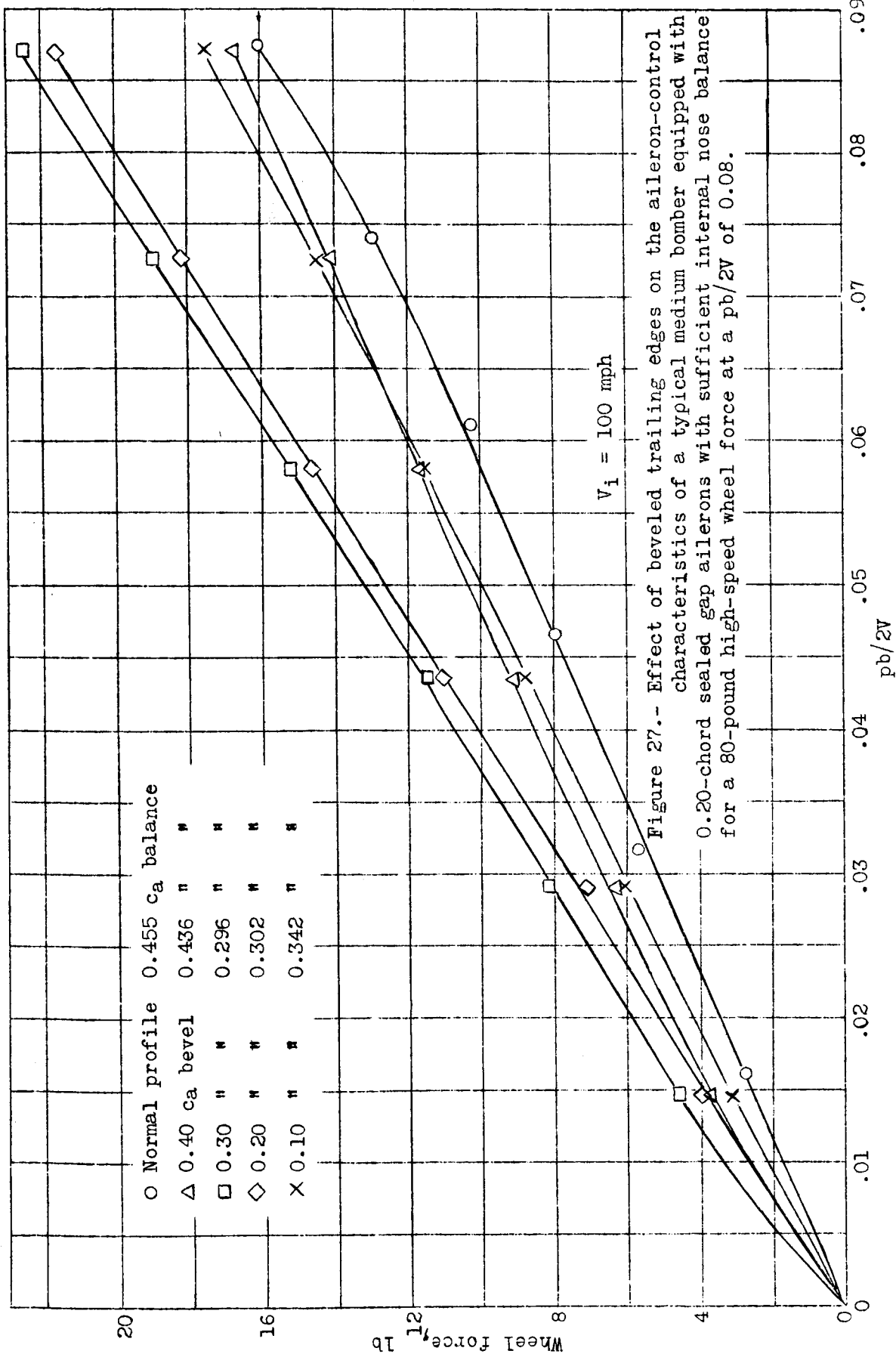


Figure 27.—Effect of beveled trailing edges on the aileron-control characteristics of a typical medium bomber equipped with 0.20-chord sealed gap ailerons with sufficient internal nose balance for a 80-pound high-speed wheel force at a $pb/2V$ of 0.08.